

Web Crippling of Rectangular Hollow section with web holes under Two Flange Loadings



By

Muhammad Amir Taimur

(Registration No: 00000362493)

Department of Structural Engineering

NUST Institute of Civil Engineering

School of Civil and Environmental Engineering

National University of Sciences & Technology (NUST)

Islamabad, Pakistan

(2024)

Web Crippling of Rectangular Hollow section with web holes under Two Flange Loadings



By

Muhammad Amir Taimur

(Registration No: 00000362493)

A thesis submitted to the National University of Sciences and Technology,
Islamabad,

in partial fulfillment of the requirements for the degree of

Master of Science in

Structural Engineering

Supervisor: Dr. Junaid Ahmad

Co Supervisor: Dr. Sarmad Shakeel

School of Civil and Environmental Engineering

National University of Sciences & Technology (NUST)

Islamabad, Pakistan

(2024)

THESIS ACCEPTANCE CERTIFICATE

It is certified that Mr. Muhammad Amir Taimur, Registration No. 00000362493, of MS Structural Engineering of batch 2021 has completed his thesis work and submitted final copy which was evaluated and found to be complete in all aspects as per policy of NUST/Regulations, is free of plagiarism, errors and mistakes and is accepted as partial fulfillment for award of MS degree. It is further certified that necessary amendments as pointed by GEC members of the scholar have been incorporated in the said thesis.

Signature: _____

Supervisor: Dr. Junaid Ahmad

Date: 29.05.2024

Signature: _____

Head of Department: Dr. Junaid Ahmad

Date: 29.05.2024

Signature: _____

Associate Dean: Dr. S. Muhammad Jamil

Date: 30/05/2024

Signature: _____

Principal & Dean (SCEE-NICE): Prof. Dr. Muhammad Irfan

Date: 30 MAY 2024

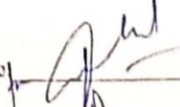
National University of Sciences and Technology

MASTER'S THESIS WORK

We hereby recommend that the dissertation prepared under our Supervision by: Muhammad Amir Taimur, Registration No. 00000362493 Titled: "Web crippling of Rectangular Hollow Section with web holes under Two Flange Loadings" be accepted in partial fulfillment of the requirements for the award of degree with B⁺ Grade.

Examination Committee Members

1. Name: Dr. Muhammad Usman

Signature: 

2. Name: Dr. Azam Khan

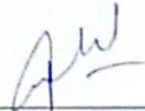
Signature: 

Co-Supervisor's Name: Dr. Sarmad Shakeel

Signature: 

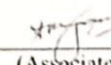
Supervisor's name: Dr. Junaid Ahmad

Signature: 



Head of Department

HeD Structural Engineering
Faculty of Civil Engineering
National University of Sciences and Technology


Dr. S. Muhammad Jamil
(Associate Dean) to Dean
NICE, SCEE, NUST

COUNTERSIGNED




PROF DR MUHAMMAD IRFAN
Principal & Dean
NICE, NUST & Dean SCEE

Date: 30 MAY 2024

CERTIFICATE OF APPROVAL

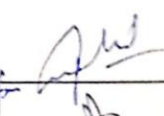
This is to certify that research work presented in this thesis, entitled "Web crippling capacity of rectangular hollow steel sections with web hole under two flange loadings" was conducted by Mr. Muhammad Amir Taimur under the supervision of Dr. Junaid Ahmad. No part of this thesis has been submitted anywhere else for any other degree. This thesis is submitted to the Department of Structural Engineering, NICE, SCEE in partial fulfillment of the requirements for the degree of Master of Science in field of Structural Engineering, Department of Structural Engineering, NICE, SCEE, National University of Sciences and Technology, Islamabad.

Student Name: Muhammad Amir Taimur


Signature 

Examination Committee:

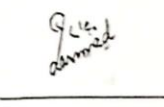
a. GEC 1: Dr. Muhammad Usman
Associate Professor,
NICE, SCEE, NUST H-12 Islamabad

Signature 

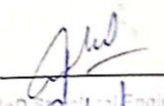
b. External Examiner 2: Dr. Azam Khan
Associate Professor,
NICE, SCEE, NUST H-12 Islamabad

Signature 

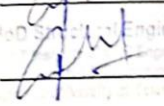
Co-Supervisor: Dr. Sarmad Shakeel,
Research Associate in Steel Structures,
Department of Civil and Structural Engineering,
Sir Frederick Mappin Building Mappin Street, Sheffield S1 3JD,
United Kingdom

Signature 

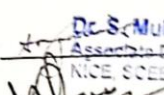
Supervisor Name: Dr. Junaid Ahmad

Signature 

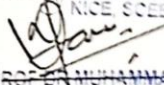
Name of HOD: *Dr Junaid Ahmad*

Signature 
Head of Department of Structural Engineering
Department of Structural Engineering
National University of Sciences and Technology

Name of Associate Dean: Dr. S. Muhammad Jamil

Signature 
Dr. S. Muhammad Jamil
Associate Dean
NICE, SCEE, NUST

Name of Principal & Dean: Dr. Muhammad Irfan

Signature 
PROF. DR. MUHAMMAD IRFAN
Principal & Dean
SCEE, NUST

AUTHOR'S DECLARATION

I Muhammad Amir Taimur hereby state that my MS thesis titled “Web crippling of Rectangular Hollow Steel Section with web holes under Two Flange Loadings” is my own work and has not been submitted previously by me for taking any degree from National University of Sciences and Technology, Islamabad or anywhere else in the country/ world.

At any time if my statement is found to be incorrect even after I graduate, the university has the right to withdraw my MS degree.

Name of Student: Muhammad Amir Taimur

Date: 30-May-24

Dedicated to my wonderful parents and sisters

ACKNOWLEDGEMENTS

I am very thankful to Almighty Allah, the most Merciful for bestowing me the dedication to complete this research work. I express my deepest gratitude for the guidance of my supervisor, Dr. Junaid Ahmad, co-supervisor Dr. Sarmad Shakeel and thesis committee members Dr. Muhammad Usman and Dr. Azam Khan, who continuously and convincingly conveyed a spirit of hard work and steadfastness to complete the project. Their valuable knowledge and insights have significantly influenced the direction of my study. Furthermore, I wish to acknowledge the exceptional contributions of Fahad Rashid from the Department of Civil Engineering, UET Peshawar, Nasim Ullah Khan from NICE, NUST, Irbaz Ahmad Khan from NICE, NUST and Raheel Asghar from Communication and Works Department, KPK. Lastly, I would like to thank the staff members of the Structural Engineering lab of NUST Institute of Civil Engineering for their assistance during experimental testing. This dissertation is a testament to the collaborative spirit and determination of all those acknowledged here and to the belief that their collective assistance was fundamental to the successful completion of my research.

TABLE OF CONTENTS

ACKNOWLEDGEMENTS	VIII
LIST OF TABLES	XI
LIST OF FIGURES	XII
LIST OF SYMBOLS, ABBREVIATIONS AND ACRONYMS	XIII
ABSTRACT	XV
CHAPTER 1: INTRODUCTION	1
1.1 Background	1
1.2 Problem Statement	5
1.3 Objectives	6
CHAPTER 2: LITERATURE REVIEW	7
2.1 Researches addressing web crippling behavior without considering web holes	7
2.1.1 W section	7
2.1.2 Channel section	8
2.1.3 Lipped channel section	9
2.1.4 Rectangular hollow section	10
2.2 Researches addressing web crippling behavior by considering web holes	11
2.2.1 W section	11
2.2.2 Channel section	12
2.2.3 Lipped channel section	12
2.2.4 Rectangular hollow section	13
2.3 Codified provisions	13
2.3.1 Specification for Structural Steel Buildings (AISC-360)	14
2.3.2 North American Specifications (AISI S100-16)	15
2.3.3 Eurocode 3: Design of steel structures	17
2.3.4 Australian standards: Steel structures (AS 4100)	18
CHAPTER 3: EXPERIMENTAL INVESTIGATION	20
3.1 Test specimens	20
3.2 Material properties	22
3.3 Bearing plates	24
3.4 Specimen labelling	24
3.5 Loading conditions and test procedure	25
CHAPTER 4: NUMERICAL INVESTIGATION	28
4.1 Finite element models	28
4.2 Geometry and material properties	29

4.3	Element type	30
4.4	Meshing	31
4.5	Interfaces	32
4.6	Boundary conditions	33
4.7	Loading procedure	34
CHAPTER 5: RESULTS, ANALYSES AND DISCUSSIONS		35
5.1	Experimental test findings	35
5.2	Comparison of finite element modelling (FEM) and experimental results	39
5.3	Parametric study	41
5.4	Web crippling strengths comparison with existing design rules	49
5.5	Proposed strength reduction factor	52
5.6	Comparison of obtained reduction factor with proposed reduction factor	53
5.6.1	Graphical depiction of comparison	53
5.6.2	Comparison using statistical analyses	57
5.7	Reliability analysis	58
CHAPTER 6: CONCLUSIONS AND FUTURE RECOMMENDATIONS		61
6.1	Conclusions	61
6.2	Future Research Recommendations	62
REFERENCES		64

LIST OF TABLES

	Page No.
Table 3.1: Material properties	23
Table 5.1: Experimentally obtained web crippling strengths.....	35
Table 5.2: Comparison of FEM and experimental results	39
Table 5.3: Web crippling strengths of specimens considered in parametric study with offset web holes under ITF loading	42
Table 5.4: Web crippling strengths of specimens considered in parametric study with offset web holes under ETF loading	43
Table 5.5 Web crippling strengths of specimens considered in parametric study with web holes positioned underneath the load bearing plates.....	44
Table 5.6: Comparisons between test and FE results of specimens without web holes with codified strengths subjected to ITF loading.....	49
Table 5.7: Comparisons between test and FE results of specimens without web holes with codified strengths subjected to ETF loading.....	50
Table 5.8: Statistical analyses of compared actual strength reduction factor with proposed strength reduction factor for (a) offset web holes (b)web holes positioned underneath load bearing plate.....	58

LIST OF FIGURES

	Page No.
Figure 3.1 X-section dimensions of test specimen	21
Figure 3.2 (a) Tested coupon (b) Dimensioned coupon.....	22
Figure 3.3: Stress-Strain curve of coupon 1.....	23
Figure 3.4: ITF loading conditions (a) Without web holes (b) With web holes	26
Figure 3.5: ETF loading conditions (a) Without web holes (b) With web holes	26
Figure 3.6: Experimental test setup for (a) ITF loading (b) ETF loading.....	27
Figure 4.1 Interfaces between bearing plate and specimen	33
Figure 4.2 Loading conditions	34
Figure 5.1: Variation of reduction factor's value of test specimens with size of web hole under (a) ITF loading (b) ETF loading	37
Figure 5.2 Variation of reduction factor's value of test specimens with position of web hole of under (a) ITF loading (b) ETF loading	38
Figure 5.3: Web crippling's failure subjected to ITF loading in (a) Experimental test specimen (b)Finite element model.....	40
Figure 5.4: Web crippling's failure mode subjected to ETF loading in (a) Experimental test specimen (b)Finite element model	41
Figure 5.5: Strength reduction variation with size of web hole for ITF loading	47
Figure 5.6 Strength reduction variation with size of web hole for ETF loading	47
Figure 5.7: Strength reduction variation with position of web hole for ITF loading.....	48
Figure 5.8: Variation of strength reduction with position of web hole for ETF loading ..	49
Figure 5.9: Comparison of strength reduction factors of specimens having offset web holes for ITF loading	54
Figure 5.10: Comparison of strength reduction factors of specimens having offset web holes for ETF loading	54
Figure 5.11: Comparison of strength reduction factors of specimen having web holes located underneath the load bearing plate for ITF loading	55
Figure 5.12: Comparison of strength reduction factors of specimen having web holes located underneath the load bearing plate for ETF loading	55
Figure 5.13 Reduction factor comparisons vs slenderness ratio for ITF loading	57
Figure 5.14 Reduction factor comparisons vs slenderness ratio for ETF loading	57

LIST OF SYMBOLS, ABBREVIATIONS AND ACRONYMS

a	Web hole diameter
A	Diameter ratio (a/h)
COV	Coefficient of variation
DL	Dead load
d	Overall depth of section
E	Elastic modulus
EOF	End-one-flange
ETF	End-two-flange
FEA	Finite element analysis
h	Flat depth of web
IOF	Interior-one-flange
ITF	Interior-two-flange
L	Specimen length
N	Bearing plate width
P	Web crippling load
P_m	Mean value of data
r_i	Radius of inside corner
r_{ext}	Radius of outer corner
R	Reduction factor
R_P	Proposed reduction factor for offset web holes
R_{PU}	Proposed reduction factor for web holes located underneath load bearing plate

<i>RHS</i>	Rectangular hollow section
<i>t</i>	Thickness of section
<i>x</i>	Offset distance of web-hole
<i>X</i>	Offset distance ratio (x/h)
β	Reliability index
ε_f	Tensile strain at fracture
\emptyset	Resistance factor
$\sigma_{0.2}$	0.2% proof stress
σ_u	Ultimate tensile strength

ABSTRACT

In this study the web crippling behavior of a hot-rolled rectangular hollow section (RHS) with web holes is demonstrated experimentally and numerically. A series of experiments were conducted to test the behavior of 20 rectangular hollow sections for web crippling strength subjected to interior-two-flange (ITF) and end-two-flange (ETF) loading conditions. The experimental program was made to get web crippling of specimen having slenderness (h/t) value of 21.32, by varying size and offset distance of web holes under two flange loading conditions. Web holes were either located centered underneath the load or at some offset distance. Finite element models of experimentally tested beams were developed, and results of finite element analysis agreed well with experimental results. A parametric study was then conducted using finite element analysis on different cross section sizes, to demonstrate the effect of size and position of web holes on web crippling capacity of rectangular hollow steel sections. The primary factors influencing the web crippling strength were determined to be the ratio of the diameter of the web hole to the depth of the flat portion of the web (a/h) and the ratio of the offset distance of the web hole to the flat portion of the web (x/h). Through the analysis, correlations were established between the ratios (a/h and x/h) and the reduction in web crippling strength. The web crippling capacities of specimens without web holes were compared to codified design provisions, and assessments were made regarding their accuracy. In both load cases, design recommendations were provided in the form of reduction factors that were both accurate and conservative. To assess the reliability of these design recommendations, reliability analyses were conducted. The results indicated that the proposed design recommendations are both safe and reliable.

Keywords: Web crippling; Rectangular hollow section; Web holes; Finite element analysis, Parametric study; Reduction factor.

CHAPTER 1: INTRODUCTION

1.1 Background

In construction engineering, the selection of material has a significant impact in determination of the safety, sustainability and cost-effectiveness of a structure. Amongst the excess of materials available, structural steel is one of the most widely used ones. Steel structure frames has been being constructed since late 19th century in response to limitation of bearing wall structures to about 10 stories height [1]. Since then, with the various advances in structural steel industry, steel became regularly used material in construction industry [2]. Usually industrial structures, tall towers, high-rise buildings and long span bridges are made up of structural steel[3]. Its high use as structural material can be attributed to its high strength to weight ratio, uniformity, elasticity, ductility toughness, speed of erection and reuse value after disassembling [4].

As a structural element, steel is predominantly utilized in two primary forms, namely hot-rolled steel and cold-formed steel. [5]. Both forms are distinguished primarily by their fabrication processes, material properties and structural applications. Hot-rolled steel sections are manufactured by rolling steel at temperatures exceeding the recrystallization temperature of the material, typically around 850 °C. This process results in steel sections with uniform material characteristics, consistent hardness, improved ductility, and minimal residual stresses. In contrast, cold-formed steel sections are created at room temperature and experience plastic deformation during the manufacturing process. This plastic deformation leads to cold-working of the material, enhancing its strength but

reducing its ductility. Variations in plastic deformation can result in non-uniform material properties and variations in hardness across the section. Hot-rolled steel sections are commonly employed as primary load-bearing structural components such as beams, columns, and braces [6], while Cold-formed steel sections are primarily utilized as secondary components, such as purlins, side rails, and cladding [7]. Extensive use of hot-rolled steel sections as primary structural element is not only attributed to the high strength and good welding performance, but also to its availability in standard sizes and shapes. They are usually available in W-shapes, Channels, Angles, Structural Tees, Pipe, Double Angles, Double Channels, and Hollow Structural Sections (HSS), as described in the AISC Steel Construction Manual [8].

Among these cross-sectional profiles, rectangular hollow section (RHS) stands out as a popular choice, primarily because of their advantageous structural properties, inbuilt aesthetic qualities, and simplicity in mass production and prefabrication [9]. When subjected to concentrated compressive load, like every other steel section rectangular hollow section is vulnerable to undergo web crippling. Web Crippling is a failure mode of web plate, in the immediate vicinity of localized concentrated load or reaction [10], [11]. The webs of steel flexural element mostly have large slenderness, Consequently, when subjected to intense localized loads or reactions, these webs are prone to experiencing crippling. This phenomenon refers to local buckling that occur in the web of a steel section under the influence of concentrated loads or reactions. This buckling occurs in the near zone of the points of load application or supports. It is distinct from global buckling, which affects the entire element, and from flange local buckling, which affects the flange elements

of the section. Web crippling has the potential to weaken the load bearing ability and structural integrity of the steel section, which may result in structural failure. The key determinants influencing the web crippling behavior of steel sections include.

Load Magnitude and Distribution: High concentrated loads, such as loads coming from point loads or reactions at supports, can cause web of section to cripple. The distribution of the load along the length of beam also plays a crucial part, with load more concentrated, more likely web crippling to occur.

Thickness of web: Steel sections having thinner webs are more prone to crippling because they have less inherent stiffness and strength. Hence, they become more susceptible to local web failure in the region closer to concentrated load.

Material Properties: The web crippling capacity of steel sections is highly affected by the mechanical properties of the steel. Steel materials with higher strengths exhibit enhanced resistance against web crippling. As different materials possess different mechanical properties, so their web crippling behavior of different materials vary from each other.

Support Conditions: The way the steel section is supported at supports, it influences the web's ability to resist crippling. Fixed supports can provide additional restraint, reducing the risk of web crippling.

Shape and dimensions of section profile: The dimensions and shape of the steel section, affect the ability of section to resist against the crippling of web. For different profiles of steel sections web crippling strength would be different. Similarly for different X-sections of same shape profile, their behavior toward web crippling varies.

Stiffeners: Presence of web stiffeners also influences the ability of steel section to resist against web crippling. By the provision of web stiffeners under the concentrated load, near the concentrated load enhances the ability of section to withstand against web crippling,

Web openings: Presence of openings in the web of steel section make a steel section more susceptible to web crippling. The size, position and configuration of the openings in the web of section influence the web crippling strength of a particular section. Various shapes of web openings like circular, rectangular or any other geometrically possible opening shape affect the web crippling strength in different way. Similarly, size and position of web holes reduces web crippling strength in different way.

Web opening is a common technique to incorporate the services within structural depth [12] These services are categorized as mechanical services, electrical services and fire safety services [13]. These services are integrated within steel structures either by suspending the services below the beam or by the provision of openings in the web of steel beam [14]. Passing services underneath the horizontal structural members results in the reduction of clear height of the floor. However, by providing openings in the web of the section ensures simpler installation and layout. Additionally, the construction zone's overall depth may be decreased accordingly, which can be advantageous for multi-story buildings that require a lot of headroom [15]. Vertically the openings are usually provided in the middle height of the web, horizontally these are either located centered under the concentrated load or at some offset distance. Despite fulfilling several functional requirements of building, these openings lead the sections more prone towards failure

because crippling of web and cause in the reduction of the web crippling strength considerably [16].

Loading condition is a critical factor that influences the web crippling strength of a section. According to AISI S100-16 [10], there are four distinct loading conditions that determine the potential for web crippling failure in steel sections. These conditions include Interior-One-Flange (IOF), End-One-Flange (EOF), Interior-Two-Flange (ITF), and End-Two-Flange (ETF) loadings. In One Flange loadings, the clear distance of the edges of adjacent opposite concentrated loads to the reactions must be at least to 1.5 times the flat depth of the section (h). On the other hand, for two flange loadings, this distance should be less than 1.5 times the flat depth of the section. Additionally, in Interior loading, the distance between the edges of bearing plate and member should exceed $1.5h$, whereas in End loading, this distance should be less than $1.5h$.

1.2 Problem Statement

Provision of openings in the web of flexural steel members provides a feasible solution for the horizontal passage of services within the steel structure. But it costs in reduction of web crippling strength of a particular section. This decrease in strength of hot-rolled multi-web sections, such as rectangular hollow sections, due to the presence of web holes, remains an area that is still unexplored. It is crucial to quantify this reduction under specified loading conditions of web crippling. To address this issue, the current study suggests an examination of the web crippling behavior of rectangular hollow sections by considering circular web holes. Through experimental and finite element investigations,

this research aims to determine the impact of the diameter and offset distance of web holes on the web crippling capacity of rectangular hollow sections.

1.3 Objectives

The major objectives of this research includes

- Experimental determination of web crippling behavior of rectangular hollow steel sections with and without consideration of circular web holes, subjected to two flange loadings.
- Numerical verification of web crippling behavior of experimentally tested specimens.
- To conduct a parametric study, considering parameters “a/h” and “x/h”.
- Assessing the impact of the size of circular web holes, positioned centrally beneath the load, on the web crippling strength of RHS.
- Evaluating the impact of the size and position of offset web holes on the web crippling behavior of RHS.

CHAPTER 2: LITERATURE REVIEW

Numerous studies have been undertaken to illustrate the structural vulnerability of various sections of hot-rolled and cold-formed steel against web crippling. During these studies several parameters like material properties, web slenderness, load bearing width, high temperature, loading conditions, fastening of flanges, web holes size and location were discussed. Also based on different researches, provisions about web crippling strength are available in different codes. These researches and codified provisions are explained in the following sections.

2.1 Researches addressing web crippling behavior without considering web holes

Various experimental and numerical researches have been carried out to demonstrate the web crippling behavior of various steel sections, excluding the consideration of web holes. These studies have looked into the impact of many parameters on the web crippling strength of section. Additionally, the web crippling strengths acquired during these researches are compared with codified provisions and conservatism or non-conservatism of codified provision is discussed. Details of these researches and their findings are explained below.

2.1.1 W section

Several studies have been carried out to investigate the web crippling behavior of W-sections. Elgaaly & Salker [17] conducted research on hot-rolled W-section under in-plane compressive loading. It was found that web crippling in slender web occurs prior to

yielding, while in stocky webs yielding occurs prior to crippling and beam, hence limit state for yielding is not necessary. Moreover, eccentric load on section can reduce the ultimate strength of section depending upon parameter like t_f/t_w and e/b_f . This reduction is hardly controlled by b_f/t_f and N/d . He and Young [18] carried out their research on cold-formed built-up W-section under all four codified loading cases. The impact of the screw's arrangement along the depth of web were inquired. It was concluded that to abstain from excessive reduction web crippling e/d ratio should not be greater than 0.3 where "e" represents the separation between the screw's center and the flange's exterior. Also, it was concluded that the currently existing codified design recommendations are either unsafe or have higher conservatism. Two design equations were presented, considering the arrangements of screw along the depth of web, and these design proposals are proved reliable and conservative.

2.1.2 Channel section

Chen et al. [5] conducted a study on the web crippling strength of hot-rolled channel sections subjected to all four load cases. Their findings revealed that the maximum web crippling capacity of channel sections occurred when the web slenderness ratio ranged between 18 and 19. Design equations were proposed for all four load cases, which were proven as safe and reliable. In a separate study, Kanthasamy et al. [19] focused on cold-formed high strength steel channel sections subjected to the ETF load case. The web crippling strengths were compared with the codified provisions and proposed equations of other researchers in the field. It was found that the currently available codified web crippling equations were overly conservative for the ETF loading condition. A web

crippling strength's design equation considering existing design provisions and a new design equation base on DSM were proposed. Both the equations are proved accurate.

2.1.3 *Lipped channel section*

Sundararajah et al.[20] conducted a study on the web crippling behavior of cold-formed lipped channel beams under two different load cases, namely IOF and EOF. The experimental web crippling strength was compared with the design rules specified in AISI S100, AS/NZ 4600, and EC3. The findings revealed that for the EOF loading condition, the design rules provided by the Australian/New Zealand standard (AS/NZS 4600) and the North American Specifications (AISI S100-16) were not conservative enough, while the predictions based on Eurocode 3 (EC 3) were overly conservative. On the other hand, for the IOF load case, the predictions from AS/NZS 4600 and AISI S100 were reasonably comparable to the experimental capacities, whereas the design rules of EC3 were excessively conservative. In a separate study by Macdonald et al. [21] the web crippling behavior of cold-formed lipped channel sections was investigated under all four load cases of web crippling. A comparison with Eurocode revealed that the predictions based on Eurocode underestimated the strength by 34% and 48% for the EOF and ETF load cases, respectively. The web crippling capacity of the lipped channel section was significantly influenced by the parameters like as bearing length, corner radii, and web depth for both IOF and EOF load cases. Nonetheless, no specific trends were observed in the case of ETF loading conditions.

2.1.4 *Rectangular hollow section*

Davies and Packer [22] conducted research on hot-rolled rectangular hollow section, subjected to transverse in-plane compressive load. It was found by increasing slenderness (d/t) of web, a generalized downward trend of web crippling capacity is observed. In addition, the web crippling strength of RHS increases linearly as bearing length (N) increases, by keeping all other conditions unchanged. A higher collapse load is observed when transferred through welded bearing plate than transferred through unwelded bearing plate. Zhou and Young [23]] conducted a research study focusing on the web crippling behavior of cold-formed stainless-steel tubular sections under two different loading conditions: end-one-flange (EOF) and interior-one-flange (IOF). The experimental web crippling load was compared with the codified design provisions for stainless steel structures, namely AISI S100-16, AS/NZ 4600, and EC3. The researchers concluded that the existing design provisions for web crippling strength in these specifications are either overly conservative or not conservative enough. To address this issue, a unified design equation was developed and presented for web crippling strength by incorporating new values coefficients, which was determined to be both safe and reliable. In a separate study, Zhan et al. [24] investigated the web crippling behavior of Lean duplex and Austenitic cold-formed stainless steel box sections under the influence of elevated temperatures. They tested a total of 21 specimens at temperatures of 20, 300, 550, and 800 °C. The findings showed that the decrease in web crippling strength for Lean-duplex RHS was slightly greater compared to austenitic stainless-steel sections at high temperatures. Additionally,

this study found that web crippling strength was not significantly affected by bearing width at elevated temperatures.

2.2 Researches addressing web crippling behavior by considering web holes

Despite having detailed literature studies about the web crippling behavior of different steel section addressing different parameters without web holes, limited researches have been conducted on section with web holes. During these researches effect of web holes in terms of size, position and edge stiffening of holes are demonstrated. These studies and their key finding are explained below.

2.2.1 W section

He and Young [25] carried out a study on cold-formed built-up W-sections by considering web holes under four different load cases: ETF, ITF, End Loading (EL), and Interior Loading (IL). The research aimed to verify the current web crippling design provisions in AISI S100–16, AS/NZS 4600, and EC3:1–3 for members that do not have web holes. By comparing the results of experimental and parametric investigations with the web crippling codified equations, it was observed that the web crippling strength determined by the existing design guidelines could be either overly conservative or unconservative. As a result, a modified unified equation was proposed by introducing a strength reduction factor for CFS built-up W-section members with and consideration of without web holes subjected to ETF, ITF, EL, and IL loading conditions. The new design proposals were found to accurately predict web crippling behavior, ensuring safety, accuracy, and reliability.

2.2.2 *Channel section*

Yousefi et al.[26] conducted a study on the web crippling behavior of cold-formed ferritic stainless steel unlipped channel sections by considering web holes under IOF and EOF loading conditions. A comparison was made between the results obtained from experiments and numerical modelling with the design guidelines of AISI S100-16. The findings revealed that the predictions provided by AISI S100-16 were overly unconservative, as much as 22%. As a result of the experimental analysis and finite element modeling, two new reduction factors were suggested.

2.2.3 *Lipped channel section*

LaBoube et al. [27] conducted an experiment where they tested a total of 108 specimens. These specimens were made up of cold-formed lipped channel sections that were interconnected with plates containing circular openings in the web. The specimens were subjected to one flange load case, the IOF and EOF load cases. The objective of the study was to determine the influence of the size and offset distance of the web holes on the web crippling strength of the section. As a result of their investigation, a web crippling reduction factor was presented for each loading condition. In a similar vein, Langan et al. [28] carried out an experiment on cold-formed C-sections. These sections had rectangular fillet corner openings and were subjected to one flange loading case. The researchers proposed an equation for the web crippling strength reduction factor for both the IOF and EOF load cases. This equation was dependent on the depth of the opening. Furthermore, Uzzaman et al. [29], [30] conducted two separate studies on cold-formed steel lipped channel sections. In one study, the sections were subjected to the ITF loading condition,

while in the other study, they were under the ETF load case. In both studies, the impact of the size and offset of the web holes on the web crippling capacity was investigated. This proposed design equations for the reduction factors specific to the ITF and ETF loadings.

2.2.4 *Rectangular hollow section*

Zhou and Young [31] carried out a series of experiments to investigate the web crippling behavior of aluminum alloy tubular sections with web holes positioned at the center under the bearing plate. The experiments were conducted under two different load cases, ITF and ETF. For each load case, a reduction factor was determined, which depended on the size of the web hole and the width of the bearing plate. The researchers proposed a design equation specifically for aluminum tubular sections with circular web openings. This design equation considered various parameters such as thickness, yield strength, ratio of bearing width to section thickness, slenderness ratio, ratio of bearing width to web flat depth, and web hole size ratio.

2.3 Codified provisions

The design guidelines pertaining to web crippling found in the current standards for steel structures are primarily empirical. These recommendations have been formulated through experimental researches carried out by various researchers from the 1940s onwards[32]. The Specification for Structural Steel Buildings (AISC-360) [11], North American Specifications (AISI S100-16) [10], Eurocode 3: Design of steel structures [33], Australian standards: Steel structures (AS 4100) are detailed below [34].

2.3.1 *Specification for Structural Steel Buildings (AISC-360)*

AISC-360 [11] defines the web crippling as the collapse of the web of steel section into buckling waves just underneath the load, occurring in webs having high slenderness ratio. Web crippling equation as shown in equation (2.1) and equation (2.2) are based on research reported by Roberts [35]. A modified equation as shown in equation (2.3) for N/d greater than 0.2 was developed after additional testing by Elgaaly and Salkar [36] to illustrate the impact of larger bearing lengths at member ends in a better way. All experiments were carried out on bare steel beam specimens, with no expectation of the advantageous effects of any floor attachments or connections. As a result, developed codified provisions are considered as safe and conservative for similar sort of utilizations. Kaczinski et al. [37] conducted experimental testing on steel box steel sections having webs of high slenderness and verified that these specifications agree well with the experimental results for this kind of member.

Based on the experimental testing findings of the aforementioned studies, the design guidelines for web crippling strength were created for bearing connections but are also broadly relevant to moment connections. Equation (2.2) and (2.3) and are desired to be applicable to the ends of beam ends where the web of the beam end is not supported, as would be the case at the end of a seated connection. When web connections are used to complete beam end connections, Equation (2.1) is used in the determination the web local crippling strength. These codified provisions as per AISC-360 are given below.

- a. When distance of load from the end of specimen is larger than or equal to $d/2$

$$0.80t_w^2 \left[1 + 3 \left(\frac{N}{d} \right) \left(\frac{tw}{tf} \right)^{1.5} \right] \sqrt{\frac{E\sigma_{0.2}t_f}{t_w}} Q_f \quad (2.1)$$

b. When distance of load from the edge of member is smaller than $d/2$

i. For N/d is less than or equal 0.2

$$0.40t_w^2 \left[1 + 3 \left(\frac{N}{d} \right) \left(\frac{tw}{tf} \right)^{1.5} \right] \sqrt{\frac{E\sigma_{0.2}t_f}{t_w}} Q_f \quad (2.2)$$

ii. For N/d is greater than 0.2

$$0.40t_w^2 \left[1 + \left(\frac{4N}{d} - 0.2 \right) \left(\frac{tw}{tf} \right)^{1.5} \right] \sqrt{\frac{E\sigma_{0.2}t_f}{t_w}} Q_f \quad (2.3)$$

Q_f is the chord stress interaction parameter, whereas the t_f and t_w are denoting thickness of the flange and web, respectively.

As per AISC-360 [11] the phenomenon of web crippling has been noted to happen in the web closer to the flange being loaded. So to mitigate the risk of web crippling failure, a three-quarter stiffener or a doubler plate or a number of stiffeners are required to be provided.

2.3.2 North American Specifications (AISI S100-16)

AISI S100-16 [10] design provisions to demonstrate the web crippling behavior of steel section on the basis of extensive experimental investigations conducted in the past studies. [38 -53]. These AISI S100-16 [10] provisions are presented in a normalized format and are dimensionless. This allows any consistent measurement system to be applicable. Fastening of test specimens with bearing plate or supports is also considered. From literature, it is concluded that the web crippling capability of

some sections varies significantly depending on way of fastening of specimen with load-bearing plate. As a result, it was determined to divide the data into groups according to whether the members were attached to the bearing plate or support. The majority of the fastening data found in the literature was derived from specimens that were bolted to the bearing plate. Practically, self-tapping screws, self-drilling screws, bolts, or welding can be used to fasten the specimen to the bearing plate. The important consideration is that, where the load applied is a crucial factor the flange parts should be prevented from rotation. The fact is that, mostly the rotation of flanges is restrained by a sheathing that is attached to them. Based on section profile in the specifications data is further distinguished by assigning data values of each section in separate table. The single web, multi web and built-up sections are considered in different tables.

Web crippling strength of any of the section (per web) is calculated as

$$C t^2 \sigma_{0.2} \sin \theta \left(1 - C_R \sqrt{\frac{r_i}{t}}\right) \left(1 + C_N \sqrt{\frac{N}{t}}\right) \left(1 - C_h \sqrt{\frac{h}{t}}\right) \quad (2.4)$$

C , C_R , C_N and C_h are general, bend radius, bearing length and web slenderness coefficients. The values of these coefficients are obtained from different tables of AISI S100-16, depending upon loading condition, section profile, fastening and unfastening of flanges.

Based on the researches [28, 54, 55] with the consideration of web holes, provisions about the web crippling C-section with web holes are presented. These design rules are applicable to any pattern of web hole that fits inside an analogous virtual hole and take into account both circular and non-circular web holes. These regulations take

into account one flange loadings (IOF and EOF) for h/t and a/h ratios up to 200 and 0.81, respectively, in the form of reduction factors. These reduction factors show that the size of the hole, as indicated by the a/h ratio, and the hole's position, as indicated by the x/h ratio, are the main determinants of the decrement in web crippling strength. Equation (2.5) provides the reduction factor, which needs to be multiplied by the web crippling strength of the specimen without web hole.

$$R_p = 1.01 - 0.325 \frac{a}{h} + 0.083 \frac{x}{h} \leq 1 \quad (2.5)$$

2.3.3 Eurocode 3: Design of steel structures

Eurocode 3 (EC3) [33] considers the web crippling behavior of steel section as section under local transverse forces. Primarily stiffening and unstiffening of web is addressed and separate design rule are provided in both cases. Design specifications are provided by considering $h_w/t \leq 200$, $r_i/t \leq 6$ and loading angle must be between 45° to 90° . Equations incorporating different coefficients are presented, for several cases of loading supports. Several load cases are designed by varying distance of load or support to free end of specimen, also distance between load and support reactions. These load cases are designed for single web sections or sections having multiple webs. The nominal web crippling strength equations for load cases resembling to ITF and ETF loading are as follows

a. For ITF loadings,

$$\frac{k_1 k_2 k_3 \left[6.66 - \frac{h/t}{64} \right] \left[1 + 0.01 \frac{N}{t} \right] t^2 \sigma_{0.2}}{\gamma_{M1}} \quad (2.6)$$

b. For ETF loadings,

$$\frac{k_3 k_4 k_5 \left[21.0 - \frac{h/t}{16.3} \right] \left[1 + 0.0013 \frac{N}{t} \right] t^2 \sigma_{0.2}}{\gamma_{M1}} \quad (2.7)$$

k_1 and k_4 are coefficients for material properties, k_2 and k_5 are coefficients for inside bend radius, whereas k_3 is the coefficient for web angle relative to flanges. Values of mentioned coefficient are calculated as explained in section 6.1.7.2 of EC3.

2.3.4 Australian standards: Steel structures (AS 4100)

In Australian standards (AS 4100) [34] expresses web crippling strength as nominal bearing strength of web plate subjected to path or concentrated loading. It is considered as the smaller value of bearing buckling strength and bearing yield strength. Considering bearing yield capacity two separate equations are used. One for rectangular or square hollow section and other for the remaining steel section. AS4100 [34] explains the dispersion of point load or load through stiff bearing lengths. This dispersion is considered to be uniform from the flange at the slope of 1: 2.5 to the flange surface. The stiff bearing length is taken as the length that cannot deform under bending. ITF and ETF loading are replicated as Interior bearing and End bearing respectively. In the interior bearing clear distance from end of load to the specimen end should be at least 1.5 times flat web depth while in case of end bearing this distance is lesser than 1.5 times flat web depth .

Equation to be used for bearing yield capacity are as follows

a. For every steel section except RHS

$$1.25Nt\sigma_{0.2} \quad (2.8)$$

b. For rectangular hollow sections

$$2b_b t \sigma_{0.2} \alpha_p \quad (2.9)$$

b_b is bearing width and calculated as the function of external radius of specimen, flat depth of web and bearing plate width. α_p is the coefficient for bearing capacity of RHS. Calculations involving b_b and α_p for ITF and ETF loading conditions are explained in section 5.13.3 of AS 4100.

From the previous studies and codified design provisions, it is noteworthy that web crippling behavior of different materials and sections has been addressed, with or without consideration of web openings. But the determination of web crippling behavior of rectangular hollow steel section with web holes, is still unexplored.

CHAPTER 3: EXPERIMENTAL INVESTIGATION

To find out the web crippling capacity of RHS with and without consideration of web holes, an experimental test program as specified in AISI S100-16 [10] was conducted under two loading conditions ITF and ETF. To get a comparison of web crippling strength one specimen for each loading condition was tested without web holes and the rest of specimens were tested for web crippling strength by changing the diameter and offset of web holes. In this way the effect of web holes size and diameter would be assessed. This experimental investigation includes selection of rectangular hollow section, preparation of test specimens for each loading condition, determination of material properties, specimen labelling and determination of web crippling strength.

3.1 Test specimens

A set of 20 experimental tests were conducted to assess the impact of web perforations on the web crippling strength of rectangular hollow sections (RHS). These tests were carried out under two distinct loading conditions, ITF and ETF. From AISC Steel Construction manual [56] a rectangular hollow section HSS 4 x 3x 3/16 was considered. The slenderness ratio (h/t) of section from its measured dimensions is calculated as 21.32. The dimensions of section were measured as, height of web (d) was 101.6 mm, depth flat portion of web (h) was 90.6 mm, width of flanges (b) was 76.2 mm, thickness of section (t) was 4.25 mm and outer radius (r_{ext}) was 5.5 mm. X-section dimension of experimental specimen is illustrated in Figure 3.1

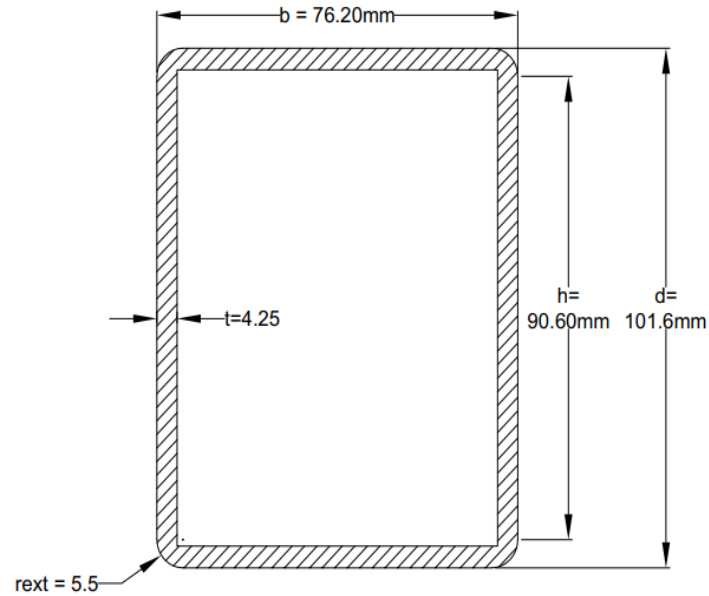


Figure 3.1 X-section dimensions of test specimen

The specimen length (L) was calculated in accordance with the guidelines presented in AISI S100-16[10], which specifies length as the clear distance between the edge of bearing plate and specimen should be at least 1.5 times the flat depth of web. Clear distance between the edge of bearing plate and specimen was provided as 1.5 times the overall section depth (d) rather than flat depth of web (h), to be conservative. In case of ITF loading, bearing plates being in the middle of specimens, clear distance is provided on both side of bearing plate. Therefore, for ITF load case the specimen's length was taken as 370 mm, by the addition of the bearing plate width (N) to clear distances on each side of bearing plate. For ETF loading length of specimen was taken as 216 mm by incorporating bearing width (N) to clear distance on one side of bearing plates as bearing plates were positioned at specimen's end. Circular web holes were provided vertically in the middle of the web having diameters (a) of 25.4 mm, 50.8 mm and 76.2 mm. Each size of web hole was located

just underneath the bearing load and at the offset distances (x) of 25.4mm and 50.8mm. Offset distance was taken as the clear distance between edge of bearing plate and web hole.

3.2 Material properties

To get the mechanical material properties of steel, two tensile coupon tests according to ASTM E8 [57] were conducted. The coupons as shown in Figure 3.2 having gauge length of 50 mm and 12.5 mm width, were prepared from the strips cut from the mid depth of web parallel to length of specimen.

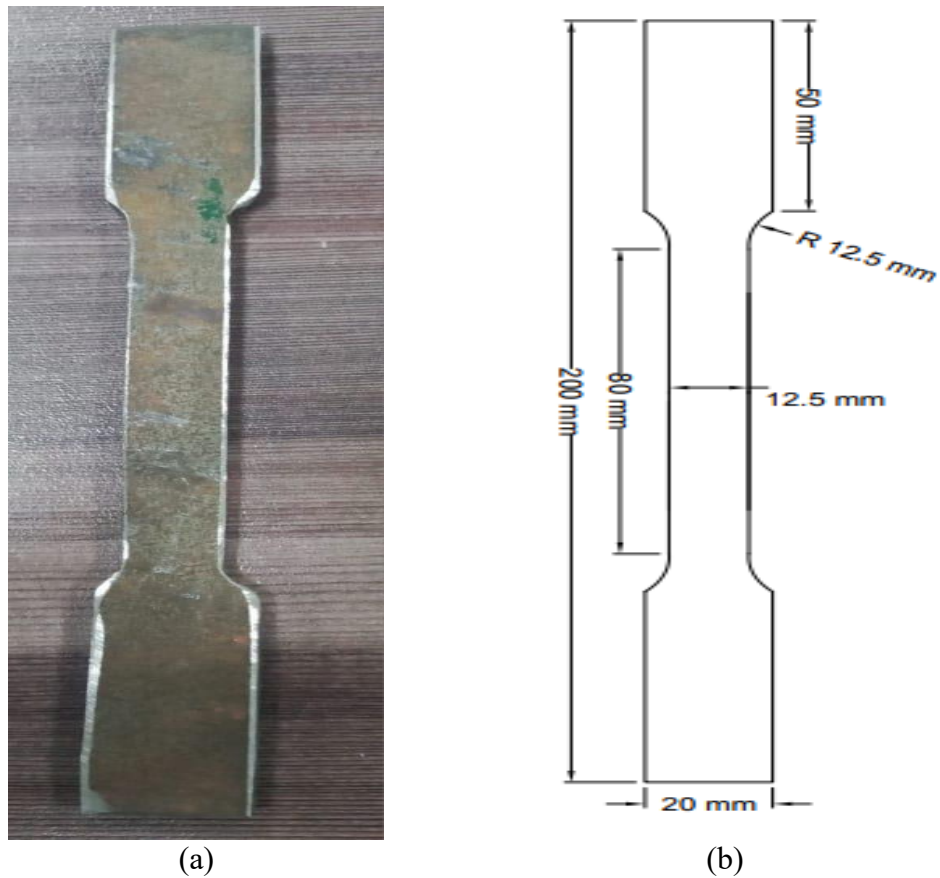


Figure 3.2 (a) Tested coupon (b) Dimensioned coupon

Tensile stresses and strains were measured based on coupons testing using a displacement-controlled Tinius-Olsen testing apparatus, and data acquisition system was utilized for the recording of results. Stress-strain curves are obtained by tensile coupon testing. Figure 3.3 displays the coupon 1 stress-strain curve.

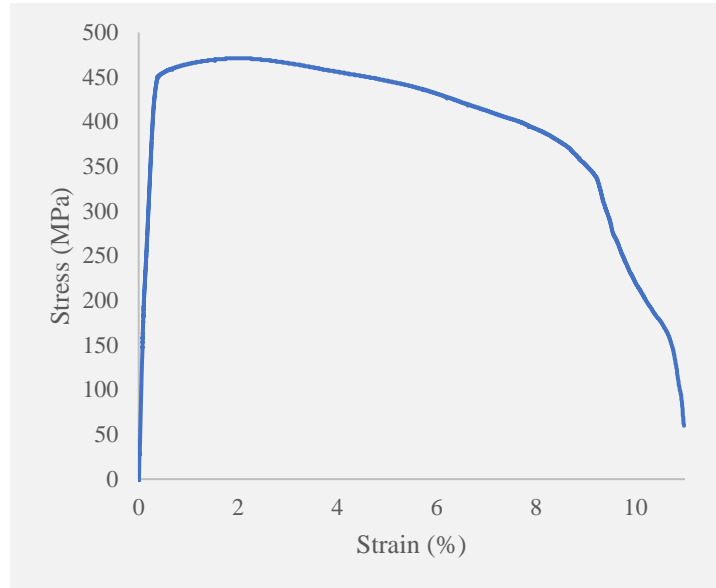


Figure 3.3: Stress-Strain curve of coupon 1

The tensile coupon tests generated stress-strain curves provided the material parameters like 0.2% proof stress ($\sigma_{0.2}$), ultimate tensile strength (σ_u), modulus of elasticity (E), fracture strain (ϵ_f). Table 3.1 provides the values of these properties.

Table 3.1: Material properties

	Material Properties			
	$\sigma_{0.2}$ (MPa)	σ_u (MPa)	E (GPa)	ϵ_f (%)
Coupon 1	450	471	202	10.98
Coupon 2	456	485	228	13.55
Mean	453	478	215	12.265

3.3 Bearing plates

Through bearing plates loading and reaction forces are applied to the specimen. Two bearing plates of similar dimensions were fabricated, one each for loading and reaction. Width of the bearing plates (N) was 63.5 mm and thickness of bearing plates was 38 mm. Length of bearing plates was made such that it should cover the whole flange width of section.

3.4 Specimen labelling

The labeling of the specimens was made in a way that the loading conditions, dimensions of specimen, ratio of diameter of web hole to the flat portion of web known as diameter ratio (a/h) and ratio of offset distance to the flat portion of web known as offset distance ratio (x/h) could be identified from specimen label. For example, “ETF-101.6 x 76.2 x 4.25 A0.27X0.55” represents the specimen as

- First three letters show load cases, either ITF or ETF load case.
- The proceeding numbers being multiplied represent the x-sectional dimension ($d \times b \times t$) of the specimen in millimeters. (101.6 x 76.2 x 4.25 stands for $d = 101.6$ mm, $b = 76.2$ mm and $t = 4.25$ mm).
- Letter “A” indicates the ratio of web hole diameter to the depth of flat portion of web plate (a/h). (A0.27 represents $a/h = 0.27$).
- Notation “X” indicates the ratio of offset distance of the web hole to the flat depth of the web (x/h). (X0.55 represents $x/h = 0.55$).

- The letter “U” in place of “X” represents that the web hole is positioned just underneath the load bearing plate.
- Notation “WH” just after the first three letters of the label indicates that the sample has no web hole subjected to that particular loading condition.

3.5 Loading conditions and test procedure

Two web crippling loading conditions were considered ITF and ETF, and specimen were tested according to procedure as specified in AISI S100-16 [10]. Figure 3.4 and Figure 3.5 shows the placement of two bearing plates, one at the top and the other below the specimen, of similar dimensions for ITF and ETF loading, respectively, at the mid-length and end of the specimen.

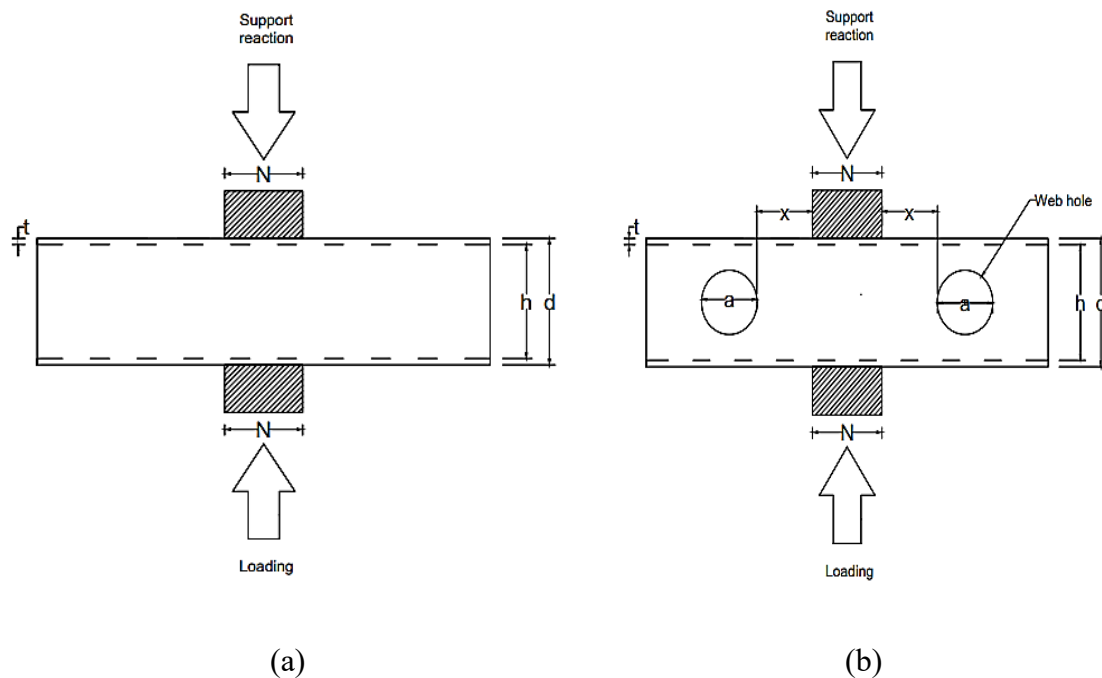


Figure 3.4: ITF loading conditions (a) Without web holes (b) With web holes

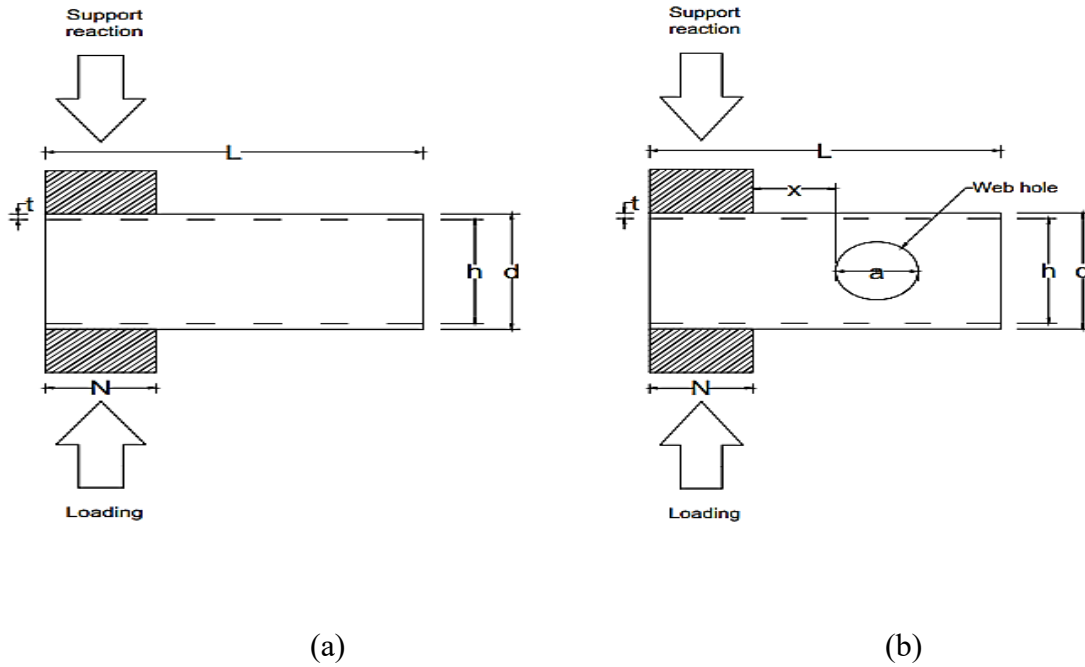


Figure 3.5: ETF loading conditions (a) Without web holes (b) With web holes

The specimen flanges were not attached to the bearing plates by any fastener. The purpose of the bottom bearing plate was to transfer the load to the specimens, while the top bearing plate was providing support., by providing reaction against the applied load. At a rate of 0.2 MPa/sec, a servo-plus hydraulic machine applied compressive load. Thus, the RHS specimen was subjected to a transverse compressive load in this testing setup. Maximum load applied to the specimen was recorded. That maximum load gives the web crippling strength value of the particular section. Figure 3.6 represents the experimental test setup for both types of loadings.



(a)

(b)

Figure 3.6: Experimental test setup for (a) ITF loading (b) ETF loading

CHAPTER 4: NUMERICAL INVESTIGATION

Numerical modeling is the practice of utilizing mathematical ideas and language to depict a physical system. It is used to describe processes at different scales which help in understanding physical processes, evaluating interactions, validating system designs, determination of the nature of problems and suggestion of solutions. In this study, numerical investigation is conducted for the validation and verification of experimental results. Finite element models are made by assigning material properties, element type, interfaces and boundary conditions to the proper geometry used in experimental investigation. The properly meshed specimen are loaded under specific boundary conditions.

4.1 Finite element models

Finite element software ABAQUS [58] was considered to create finite element models of experimentally tested specimens. With its foundation in the finite element method, ABAQUS is a strong engineering simulation suite. In structural and civil engineering, it is widely considered for performing both linear and nonlinear analysis of structures and components. Because of its advanced simulation capabilities robustness and versatility, it stands out as a leading finite element analysis (FEA) program. It empowers researchers to model and analyze complex real-world problems, optimize designs, and innovate across various fields, ensuring safety, performance, and reliability of products and structures.

X-dimensions and the material characteristics of the specimen determined through the experimental test investigations were specified in the modeling of the finite element models of the experimentally tested specimens. By modelling rectangular hollow sections and bearing plates and by assigning interfaces between bearing plates and specimen and proper boundary conditions for each loading condition, the experimental test setup was replicated in finite element program.

4.2 Geometry and material properties

Specimens were modeled using dimensions of test specimens. To assign material properties to sections, the stress-strain curve of the coupon test was utilized. The material properties of coupon 1 were assigned. For the analysis in the elastic region 0.2 percent proof stress and elastic modulus values are assigned. The Poisson's ratio value was specified as 0.3. The value of Poisson's ratio was adopted from literature. [59, 60]. By assigning the true stress and true plastic strain values according to ABAQUS manual [58], material non-linearity was specified to ascertain the plastic behavior of each model under consideration. These true stress and plastic strain values are calculated as shown in equation (4.1) and (4.2).

$$\varepsilon_t = \ln(1 + \varepsilon_e) \quad (4.1)$$

$$\sigma_t = \sigma_e(1 + \varepsilon_e) \quad (4.2)$$

ε_t , σ_t , ε_e and σ_e are true strain, true stress, engineering strain and engineering stress, respectively. Engineering stress and strain value are obtained from the stress strain curve generated by tensile coupon test. These are calculated on the basis of initial original

area of coupon. True stress and strain values incorporate the actual area at every instant of time.

4.3 Element type

For the modelling rectangular hollow steel sections S4R shell elements is adopted. The S4R element features hourglass control, reduced integration, and finite membrane strains. It is a four-node thick or thin doubly curved shell element. It has been effectively utilized in prior research conducted on hot-rolled steel sections [61, 62] and performed well for web crippling numerical studies too [63, 64, 65]. It is considered suitable for complex buckling behavior according to ABAQUS manual [58].

The hour-glass control technique of S4R shell element is used to mitigate hourglass modes, which are non-existing modes of those may exist in reduced integration elements, more specifically in 3D modeling. These modes are associated with zero-energy deformation patterns that do not correspond to realistic physical behavior, causing inaccurate results in the finite element analysis. Effective hourglass control plays a key part in ensuring the accuracy and stability of simulations, particularly when using reduced integration elements in complex models. Reduced integration technique makes use of fewer integration points compared to full integration. Because of this, fewer calculations are required. As a result, computation time reduces which makes it attractive for large-scale models and nonlinear analyses. Finite element strains property of S4R shell element in finite element analysis (FEA) and structural mechanics accounts for large deformations and rotations that occur in the structure.

To model bearing plate discrete rigid solid element is used. This element does not undergo deformation under the action of applied load. Hence this bearing plate modelled by discrete rigid solid element transfers the load well to the specimen and resists the load as support well. Also, during modelling of this element, material properties are not required to provide.

4.4 Meshing

To obtain accurate results in less computation time, mesh sensitivity analyses were performed on different models for each loading condition. During mesh sensitivity analysis different sizes of the mesh were adopted and kept on reducing. The sizes of mesh for which results converge close to each other, that mesh size was considered and used for that particular loading conditions. Based on mesh sensitivity analysis RHS models subjected to ITF loading were meshed of size of $4 \times 4 \text{ mm}^2$, while for ETF models $3 \times 3 \text{ mm}^2$ mesh size was adopted. The meshing size of the bearing plate was $10 \times 10 \text{ mm}^2$. To obtain a proper and well-structured mesh, Mesh control was assigned to the finite element models. In mesh controls quad shaped element, free technique and medial axis algorithm with minimized meshed transition was specified.

The free meshing technique is a flexible method used to generate a mesh for complex geometries. It can handle highly irregular and intricate geometries. Free meshing is adopted when it is required to analyze complex and free-form geometries. Applying this technique to individual parts, regions, or model, ensures that even the most complicated shapes are properly meshed. The medial axis algorithm is a specialized meshing technique that focuses on the geometric and topological skeleton of a model to create a high-quality

mesh. This option is usually opted for geometries where a high-quality, well-structured mesh is needed but the geometry does not shape itself to standard structured meshing techniques. ABAQUS [58] will use the medial axis to guide the meshing process, providing better element quality. In this modelling, free technique and medial axis algorithm is adopted in controlled mesh option to get a high quality and well-shaped mesh around the circular web openings and at the filleted corner of rectangular hollow specimen.

4.5 Interfaces

To make a web crippling test of rectangular hollow section, interfaces between the bearing plate and RHS specimen were assigned. As RHS specimen and bearing plates were in contact with each other. Thus, surface to surface contact was considered to assign the interfaces between the specimen and the bearing plates. The Surface of bearing plates in contact with specimen was assigned as master surface, however rectangular hollow section was regarded as the slave surface. Penetration of contact surfaces was not allowed. Hard contact was assigned and friction coefficient between bearing plate and steel section was taken as 0.4, as specified in different studies for friction coefficient [66, 67, 68].

The concept of master and slave surface is important for defining how two surfaces interact with each other. The surface which is more rigid or less deformable in a contact pair is usually considered as master surface. It is assigned to the larger, stiffer, or more geometrically significant part of the model. The slave surface is typically the more flexible or deformable surface in a contact pair. It is often assigned to the smaller, more compliant part of the model. The master surface dictates the contact constraints, while the slave surface conforms to these constraints, ensuring accurate and realistic simulation of contact

interactions. Properly defining these surfaces of key importance for achieving reliable and accurate results in finite element analyses involving contact mechanics. So the top surface of bottom bearing plate and bottom surface of top bearing plate are considered as master surface and rectangular hollow section is considered as slave surface in this modelling as demonstrated in Figure 4.1

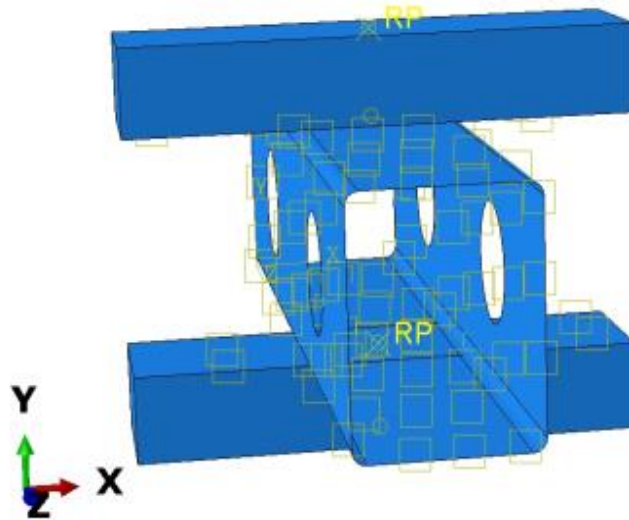


Figure 4.1 Interfaces between bearing plate and specimen

4.6 Boundary conditions

For the boundary condition, reference points were specified at top and bottom bearing plates. Replicating experimental testing procedure, the upper bearing plate was effectively constrained in all directions to offer support against the applied load. This was achieved by setting the reference point on the upper bearing plate to have zero displacement and rotation. However, the bottom bearing plate was not restricted in the vertical direction, which was the only degree of freedom not constrained. These specified boundary conditions are represented in Figure 4.2.

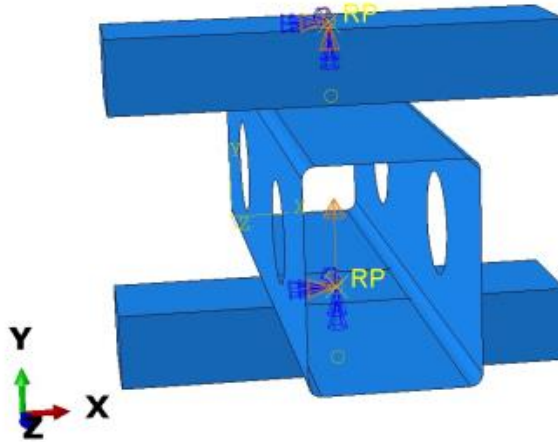


Figure 4.2 Loading conditions

4.7 Loading procedure

Compressive load was applied to the rectangular hollow sections in the transverse direction by assigning displacement in the vertical direction to the reference point located on the bottom bearing plate. Generally, 1 to 2 mm displacement in the upward direction was specified. In this way because of the specified vertical translation of bottom bearing plate, transverse load was applied. So due of the application of transverse load from bottom bearing plate and support at top bearing plate, web crippling behavior of the rectangular hollow section's model was observed, by running the job. A load deformation curve was obtained as a result of analysis. Maximum value of load gives the value of web crippling strength.

CHAPTER 5: RESULTS, ANALYSES AND DISCUSSIONS

As a result of experimental tests investigation and analysis of numerical modelling, web crippling strengths of specimen with and without consideration of web holes are observed. The subsequent sections present tabulated representation of these strengths, graphical depictions of the decrement in strength because of web holes, and comprehensive analyses of these findings.

5.1 Experimental test findings

A set of 20 tests were experimentally conducted, with 10 under each loading condition ITF and ETF. The web crippling strengths of the specimens, encompassing both webs are tabulated in Table 5.1 for both ITF and ETF loadings.

Table 5.1: Experimentally obtained web crippling strengths

Loading condition	Specimen	Web crippling Strength (KN)	Reduction factor (R)
ITF	ITF-101.4 x 76.2 x 4.25 WH	309.45	
	ITF-101.4 x 76.2 x 4.25 A0.27U	249.72	0.81
	ITF-101.4 x 76.2 x 4.25 A0.27X0.27	290.76	0.94
	ITF-101.4 x 76.2 x 4.25 A0.27X0.55	301.21	0.97
	ITF-101.4 x 76.2 x 4.25 A0.55U	239.02	0.77
	ITF-101.4 x 76.2 x 4.25 A0.55X0.27	276.63	0.89
	ITF-101.4 x 76.2 x 4.25 A0.55X0.55	294.86	0.95
	ITF-101.4 x 76.2 x 4.25 A0.83U	195.06	0.63
	ITF-101.4 x 76.2 x 4.25 A0.83X0.27	265.77	0.86
	ITF-101.4 x 76.2 x 4.25 A0.83X0.55	290.90	0.94
ETF	ETF-101.4 x 76.2 x 4.25 WH	199.37	
	ETF-101.4 x 76.2 x 4.25 A0.27U	160.54	0.81
	ETF-101.4 x 76.2 x 4.25 A0.27X0.27	181.70	0.91
	ETF-101.4 x 76.2 x 4.25 A0.27X0.55	192.31	0.96

ETF-101.4 x 76.2 x 4.25 A0.55U	140.61	0.71
ETF-101.4 x 76.2 x 4.25 A0.55X0.27	180.88	0.91
ETF-101.4 x 76.2 x 4.25 A0.55X0.55	191.93	0.96
ETF-101.4 x 76.2 x 4.25 A0.83U	116.83	0.59
ETF-101.4 x 76.2 x 4.25 A0.83X0.27	173.55	0.87
ETF-101.4 x 76.2 x 4.25 A0.83X0.55	183.93	0.92

From the finding of experimental investigations, it is noted that the web crippling capacities of ITF specimens are higher than those of ETF loading. It is because of the reason that in ITF loading there exists the span of specimen on each side of loading while leads the ITF specimen to withstand more loads. In case of ETF loadings there is a span only one side and load is being applied at the other end of specimen. So, resistance against its web crippling become lesser. The ratio of strengths for ITF to the ETF loading for different specimen ranged from 1.53 to 1.70. Web crippling strength of specimen after reduction because of web holes is expressed by reduction factor “R”. It is calculated as the ratio of web crippling strength of a particular specimen having web holes to the web crippling strength of specimen without considering web holes. Experimental results show that by increasing the size of web hole, value of R decreases indicating that there would be higher strength reduction. Conversely, by changing the position of web holes from centered under the load bearing plate to an offset distance, R value increases showing that with increase in offset distance, reduction in web crippling strength would be lesser. For a specific size of web hole, when the web holes are positioned centered underneath the load bearing plate, web crippling’s strength reduction is highest. It is found that for web holes located under load bearing plate is web crippling strength reduction trend in case of web holes is steeper as compared to offset web hole.

Effect of size of web holes is demonstrated in

Figure 5.1. It has been noted that as the diameter of web holes is increasing in the form of increased a/h value, R value decreases for both the loading conditions. The decline in R value indicates that web crippling strength is decreasing. This decrease trend is not very high in case of specimen with offset web holes. These specimens with offset web holes in the graphs of Table 5.1 are 101.6 x 76.2 x 4.25 X0.27 and 101.6 x 76.2 x 4.25 X0.55 subjected to both loading conditions. For the specimens 101.6 x 76.2 x 4.25 U under the both loading conditions web holes are located centered underneath the web hole. For these specimens by increasing the size of web holes results in the significant enhancement in the decrement of web crippling strength

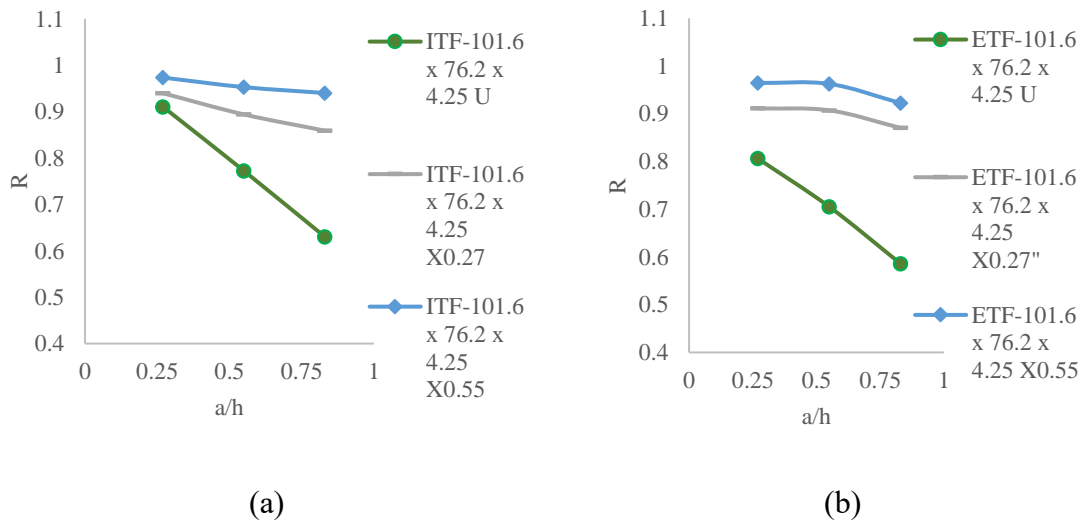


Figure 5.1: Variation of reduction factor's value of test specimens with size of web hole under (a) ITF loading (b) ETF loading

Effect of position of web holes is shown in Table 5.2. It is found that under both loading conditions ITF and ETF, with increase in the offset distance in the form of

increased x/h value, R value increases. The upward movement in the R value indicates that web crippling strength is increasing by increasing offset distance. The increase trend in all the three graphs shown in Table 5.2 are almost similar each loading condition. In this trend initially high increase in web crippling strength is observed by moving from U to x/h value of 0.27. After moving from x/h value of 0.27 to 0.55 web crippling strength increases at lower rate. It indicates that the reduction rate in case of web holes centered underneath the load is more as compared to offset web holes. Similarly, the gap between different points at U representing the specimen with web holes located underneath the load bearing plates is more as compared to points representing specimen having offset web holes. It shows that by increasing size of web holes when web holes are located underneath the web holes, reduction would be more as compared to offset web holes.

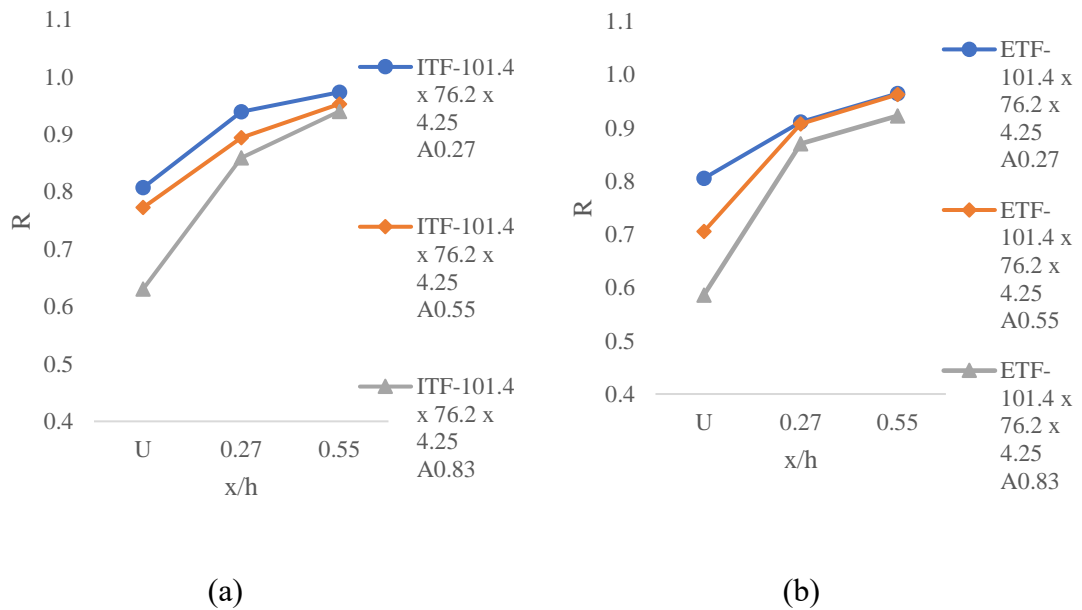


Figure 5.2 Variation of reduction factor's value of test specimens with position of web hole of under (a) ITF loading (b) ETF loading

5.2 Comparison of finite element modelling (FEM) and experimental results

The experimental failure loads against web crippling tests are compared with the failure loads obtained by numerical modelling to validate the numerical models. This comparison is shown in Table 5.2. The mean values (P_m) of the ratio of experimental to the finite element analysis web crippling load, P_{EXP}/P_{FEA} were 0.98 and 1.03, and coefficients of variation (V_P) were 0.052 and 0.069 for ITF and ETF loading conditions respectively. In ITF loading condition, a maximum of 12% variation is observed in case of ITF-101.6 x 76.2 x 4.25 A0.83U. For ETF loading, maximum of 13 % variation was found between the ETF-101.6 x 76.2 x 4.25 A0.83U numerical and experimental results. Here the mean values and coefficients of variation of P_{exp}/P_{FEA} indicate that finite element models are very closely predicting the web crippling strength of RHS with and without consideration if web holes for both the loading conditions.

Table 5.2: Comparison of FEM and experimental results

Specimen	P_{FEA} (kN)		P_{exp}/P_{FEA}	
	ITF	ETF	ITF	ETF
101.6 x 76.2 x 4.25 WH	291.27	200.4	0.94	1.01
101.6 x 76.2 x 4.25 A0.27U	259.55	168.5	1.04	1.05
101.6 x 76.2 x 4.25 A0.27X0.27	287.45	197.55	0.99	1.09
101.6 x 76.2 x 4.25 A0.27X0.55	290.4	200.15	0.96	1.04
101.6 x 76.2 x 4.25 A0.55U	223.55	135.13	0.94	0.96
101.6 x 76.2 x 4.25 A0.55x0.27	282.37	196.98	1.02	1.09
101.6 x 76.2 x 4.25 A0.55x0.55	289.26	199.41	0.98	1.04
101.6 x 76.2 x 4.25 A0.83U	172.1	101.85	0.88	0.87
101.6 x 76.2 x 4.25 A0.83X0.27	278.29	192.46	1.05	1.11
101.6 x 76.2 x 4.25 A0.83X0.55	287.75	198.17	0.99	1.08
Mean, P_m			0.98	1.03
Coefficient of variation, V_P			0.052	0.069

Comparison of web crippling failure mode between experimental and numerical analysis web crippling for ITF loading is shown in Figure 5.3. From the ITF deformed shapes of experimental specimen, it observed that crumpling of web into wave form is found at the center of the specimen under the load bearing plate. This crumpling originates vertically from the center of the web, and it extends till the web holes. In the numerical model too, a higher intensity of web is observed in mid depth of the of web till area around web holes. And shapes of web crippling failure are similar in experimental specimen and numerical model

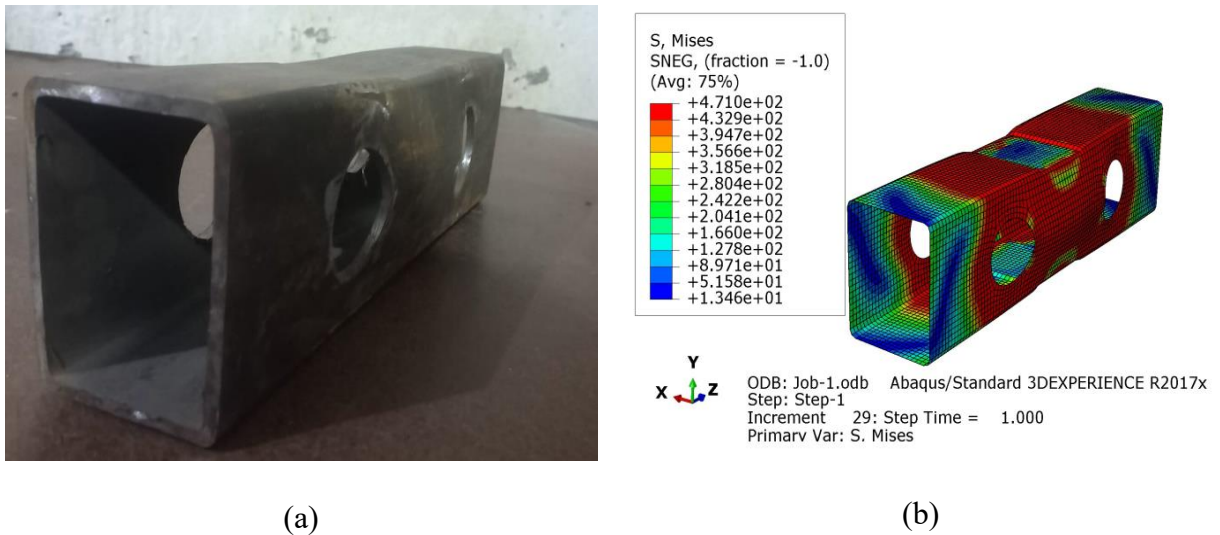


Figure 5.3: Web crippling’s failure subjected to ITF loading in (a) Experimental test specimen (b)Finite element model

Comparison of failure modes of experimental specimen and numerical model for ETF loading is shown in Table 5.4. In ETF failure modes web crippling is observed at the end of beam underneath the load bearing plate and it extends till web holes in both experimental specimen and numerical model. In this case too stress intensity is found most at the end of specimen underneath the load and higher intensity S. Mises stress concentration is found in the area around web holes. The extension of web crumpling from

underneath the load till web hole and stress intensity around web holes indicate that web openings are participating in inducing the web crippling failure of the particular section.

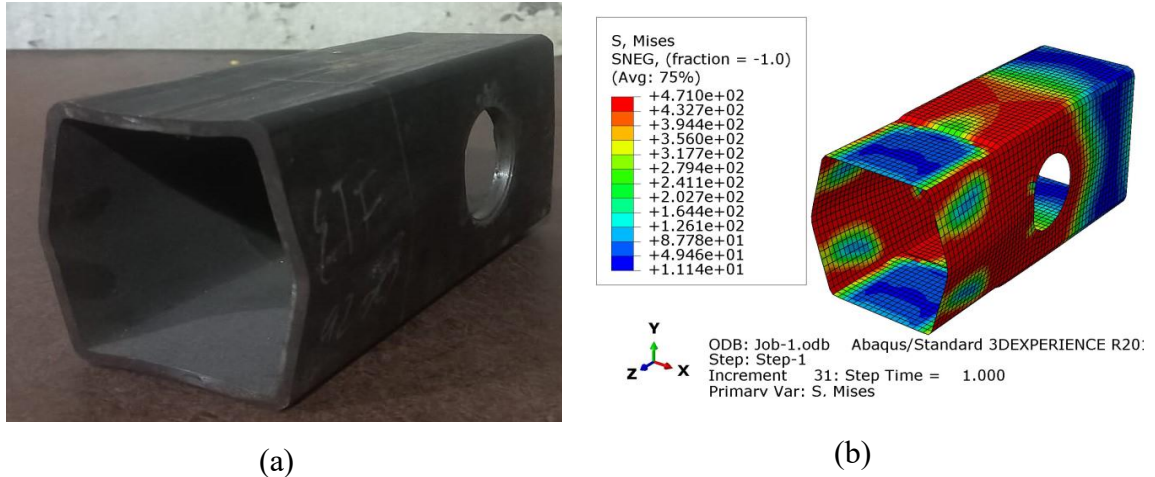


Figure 5.4: Web crippling’s failure mode subjected to ETF loading in (a) Experimental test specimen (b)Finite element model

For both loading conditions, the numerical model's crippling failure modes are the same as the failure modes identified in experiments. Numerical values are sufficiently similar to the experimental web crippling strength, according to a comparison of experimental and FEA results. In the same way, numerical model failure modes resemble experimental failure modes. Thus, it can be deduced that these numerical models are predicting the web crippling behavior of experimentally tested RHS specimen with web holes under both loading conditions effectively. Hence, considering the strength and failure mode of web crippling, a satisfactory concurrence is achieved between the findings from experiments and numerical simulations.

5.3 Parametric study

ABAQUS [58] created finite element models closely predicts the web crippling failure mode and strengths of rectangular hollow sections considering web holes under both

loading cases. Based on the verification of numerical results with experimental results, an investigation was carried out to analyze the impact of web holes on the web crippling behavior of rectangular hollow sections through a parametric study. For this parametric study, six different sections having thickness ranging from 2.94 to 11.81 mm were considered. The slenderness ratio (h/t) of these specimens were ranging from 9.99 to 58.43. The rectangular hollow sections under consideration during this parametric study are as follows.

- HSS 5 x 4 x 3/16
- HSS 7 x 5 x 1/8
- HSS 10 x 5 x 3/16
- HSS 5 x 4 x 3/16
- HSS 7 x 5 x 1/8
- HSS 10 x 5 x 3/16

The Diameter ratio (a/h) were 0.2, 0.27, 0.4, 0.55 and 0.83 and for the specimen with offset web holes, Offset distance ratio (x/h) were 0.2, 0.27, 0.4, 0.55 and 0.8. The bearing plate with a width of 63.5 mm was used for specimens of sections 127 x 101.6 mm and 177.8 x 127 mm. For the section of 254 x 127mm, a 90 mm wide bearing plate was considered. The material properties (0.2 percent proof stress, ultimate stress, elastic modulus and true stress and strain value), element type, interfaces, boundary condition and loading procedure were similar to that of previous numerical models of experimentally tested beam.

Table 5.3: Web crippling strengths of specimens considered in parametric study with offset web holes under ITF loading

Specimen	h/t	L (mm)	P_{FEA} (kN)				
			X0.2	X0.27	X0.4	X0.55	X0.8
ITF-127 x 101.6 x 4.42 A0.2	26.70	450	332.11	333.08	335.77	336.91	339.08
ITF-127 x 101.6 x 4.42 A0.27	26.70	450	329.20	330.74	332.64	333.33	334.36

ITF-127 x 101.6 x 4.42 A0.4	26.70	450	325.86	327.78	330.39	331.23	332.36
ITF-127 x 101.6 x 4.42 A0.55	26.70	450	320.03	323.66	327.94	330.03	331.19
ITF-127 x 101.6 x 4.42 A0.83	26.70	450	315.89	320.71	323.56	327.31	330.45
ITF-127 x 101.6 x 11.81 A0.2	9.99	450	1450.49	1455.23	1458.07	1460.61	1464.48
ITF-127 x 101.6 x 11.81 A0.27	9.99	450	1437.95	1443.74	1447.84	1458.76	1460.12
ITF-127 x 101.6 x 11.81 A0.4	9.99	450	1387.61	1406.30	1430.91	1438.76	1446.35
ITF-127 x 101.6 x 11.81 A0.55	9.99	450	1321.41	1357.71	1416.62	1428.85	1438.77
ITF-127 x 101.6 x 11.81 A0.83	9.99	450	1243.79	1293.99	1366.53	1394.53	1430.65
ITF-177.8 x 127 x 2.94 A0.2	58.44	650	162.04	163.14	165.33	168.61	170.00
ITF-177.8 x 127 x 2.94 A0.27	58.44	650	156.47	158.09	161.62	164.75	169.05
ITF-177.8 x 127 x 2.94 A0.4	58.44	650	146.28	149.21	156.07	162.75	169.40
ITF-177.8 x 127 x 2.94 A0.55	58.44	650	135.01	142.15	151.97	159.97	168.21
ITF-177.8 x 127 x 2.94 A0.83	58.44	650	121.15	135.50	147.99	157.30	166.65
ITF-177.8 x 127 x 8.86 A0.2	19.39	650	1016.08	1017.60	1020.49	1030.77	1038.34
ITF-177.8 x 127 x 8.86 A0.27	19.39	650	1006.18	1013.03	1017.94	1019.95	1021.45
ITF-177.8 x 127 x 8.86 A0.4	19.39	650	973.45	999.10	1010.77	1016.00	1020.20
ITF-177.8 x 127 x 8.86 A0.55	19.39	650	939.48	978.11	998.58	1007.04	1017.90
ITF-177.8 x 127 x 8.86 A0.83	19.39	650	910.71	970.44	985.44	1001.75	1012.23
ITF-254 x 127 x 4.42 A0.2	55.43	900	361.06	363.56	370.17	373.49	374.80
ITF-254 x 127 x 4.42 A0.27	55.43	900	348.11	352.78	364.44	372.27	374.71
ITF-254 x 127 x 4.42 A0.4	55.43	900	316.42	332.18	353.99	359.99	370.03
ITF-254 x 127 x 4.42 A0.55	55.43	900	297.13	319.26	346.08	352.39	368.53
ITF-254 x 127 x 4.42 A0.83	55.43	900	270.83	302.31	337.85	349.40	367.47
ITF-254 x 127 x 7.39 A0.2	33.15	900	921.85	937.78	940.35	942.58	944.16
ITF-254 x 127 x 7.39 A0.27	33.15	900	909.27	922.46	928.58	932.52	935.82
ITF-254 x 127 x 7.39 A0.4	33.15	900	837.77	895.79	918.83	927.70	933.67
ITF-254 x 127 x 7.39 A0.55	33.15	900	747.84	850.20	899.90	920.49	930.61
ITF-254 x 127 x 7.39 A0.83	33.15	900	707.82	776.59	884.25	909.76	928.58

Table 5.4: Web crippling strengths of specimens considered in parametric study with offset web holes under ETF loading

Specimen	h/t	L (mm)	P _{FEA} (kN)				
			X0.2	X0.27	X0.4	X0.55	X0.8
ETF-127 x 101.6 x 4.42 A0.2	26.70	254	237.08	238.98	241.94	244.60	247.09
ETF-127 x 101.6 x 4.42 A0.27	26.70	254	234.77	235.66	238.66	241.21	243.92
ETF-127 x 101.6 x 4.42 A0.4	26.70	254	219.69	226.46	233.67	237.98	239.21

ETF-127 x 101.6 x 4.42 A0.55	26.70	254	216.97	219.09	225.41	233.36	235.96
ETF-127 x 101.6 x 4.42 A0.83	26.70	254	206.29	211.05	219.81	224.21	230.44
ETF-127 x 101.6 x 11.81 A0.2	9.99	254	961.46	963.46	966.08	967.21	969.32
ETF-127 x 101.6 x 11.81 A0.27	9.99	254	957.89	959.86	963.73	965.09	967.22
ETF-127 x 101.6 x 11.81 A0.4	9.99	254	943.79	949.35	953.01	955.70	958.56
ETF-127 x 101.6 x 11.81 A0.55	9.99	254	925.36	941.13	946.92	948.57	955.28
ETF-127 x 101.6 x 11.81 A0.83	9.99	254	904.96	909.06	923.08	928.99	934.15
ETF-177.8 x 127 x 2.94 A0.2	58.44	350	89.29	89.61	90.17	90.75	91.25
ETF-177.8 x 127 x 2.94 A0.27	58.44	350	87.18	88.41	89.95	90.53	90.96
ETF-177.8 x 127 x 2.94 A0.4	58.44	350	85.23	86.98	88.91	89.73	90.55
ETF-177.8 x 127 x 2.94 A0.55	58.44	350	83.48	85.34	87.91	89.24	90.43
ETF-177.8 x 127 x 2.94 A0.83	58.44	350	81.98	83.52	86.38	88.00	89.66
ETF-177.8 x 127 x 8.86 A0.2	19.39	350	678.64	683.46	685.95	686.54	689.05
ETF-177.8 x 127 x 8.86 A0.27	19.39	350	676.42	679.14	681.21	684.56	685.86
ETF-177.8 x 127 x 8.86 A0.4	19.39	350	667.27	674.22	678.01	681.39	684.99
ETF-177.8 x 127 x 8.86 A0.55	19.39	350	665.62	671.08	674.93	678.16	683.32
ETF-177.8 x 127 x 8.86 A0.83	19.39	350	652.66	662.48	666.61	673.36	680.84
ETF-254 x 127 x 4.42 A0.2	55.43	500	229.53	230.88	231.66	232.45	232.94
ETF-254 x 127 x 4.42 A0.27	55.43	500	226.64	228.30	231.00	231.01	231.73
ETF-254 x 127 x 4.42 A0.4	55.43	500	221.77	223.77	225.48	229.35	230.94
ETF-254 x 127 x 4.42 A0.55	55.43	500	218.25	221.14	222.70	226.45	229.11
ETF-254 x 127 x 4.42 A0.83	55.43	500	212.97	216.83	220.23	224.14	227.15
ETF-254 x 127 x 7.39 A0.2	33.15	500	585.67	586.95	587.94	588.05	589.01
ETF-254 x 127 x 7.39 A0.27	33.15	500	576.65	578.16	580.25	581.14	582.48
ETF-254 x 127 x 7.39 A0.4	33.15	500	573.66	575.78	578.78	580.79	581.34
ETF-254 x 127 x 7.39 A0.55	33.15	500	568.85	570.98	573.29	574.58	577.63
ETF-254 x 127 x 7.39 A0.83	33.15	500	554.73	560.68	565.13	572.21	577.35

Table 5.5 Web crippling strengths of specimens considered in parametric study with web holes positioned underneath the load bearing plates

Section	h/t	L (mm)		P _{FEA} (kN)	
		ITF	ETF	ITF	ETF
127 x 101.6 x 4.42 A0.2U	26.70	450	254	329.53	225.25
127 x 101.6 x 4.42 A0.27U	26.70	450	254	318.02	197.32
127 x 101.6 x 4.42 A0.4U	26.70	450	254	296.12	176.77
127 x 101.6 x 4.42 A0.55U	26.70	450	254	255.96	158.54
127 x 101.6 x 4.42 A0.83U	26.70	450	254	179.85	111.18

127 x 101.6 x 11.81 A0.2U	9.99	450	254	1392.75	935.82
127 x 101.6 x 11.81 A0.27U	9.99	450	254	1343.62	827.59
127 x 101.6 x 11.81 A0.4U	9.99	450	254	1261.06	737.98
127 x 101.6 x 11.81 A0.55U	9.99	450	254	1101.81	672.38
127 x 101.6 x 11.81 A0.83U	9.99	450	254	821.79	485.39
177.8 x 127 x 2.94 A0.2U	58.44	450	254	160.85	79.99
177.8 x 127 x 2.94 A0.27U	58.44	450	254	152.47	73.78
177.8 x 127 x 2.94 A0.4U	58.44	650	350	135.41	70.99
177.8 x 127 x 2.94 A0.55U	58.44	650	350	117.39	66.52
177.8 x 127 x 2.94 A0.83U	58.44	650	350	82.91	48.44
177.8 x 127 x 8.86 A0.2U	19.39	650	350	975.19	619.30
177.8 x 127 x 8.86 A0.27U	19.39	650	350	924.86	572.91
177.8 x 127 x 8.86 A0.4U	19.39	650	350	846.92	507.25
177.8 x 127 x 8.86 A0.55U	19.39	650	350	753.84	425.36
177.8 x 127 x 8.86 A0.83U	19.39	650	350	491.13	290.81
254 x 127 x 4.42 A0.2U	55.43	650	350	363.54	190.30
254 x 127 x 4.42 A0.27U	55.43	650	350	345.41	174.97
254 x 127 x 4.42 A0.4U	55.43	650	350	307.79	170.83
254 x 127 x 4.42 A0.55U	55.43	650	350	267.54	159.09
254 x 127 x 4.42 A0.83U	55.43	900	500	186.97	115.92
254 x 127 x 7.39 A0.2U	33.15	900	500	895.35	483.91
254 x 127 x 7.39 A0.27U	33.15	900	500	846.56	473.98
254 x 127 x 7.39 A0.4U	33.15	900	500	735.77	466.57
254 x 127 x 7.39 A0.55U	33.15	900	500	655.67	420.98
254 x 127 x 7.39 A0.83U	33.15	900	500	446.48	278.09

Table 5.3, Table 5.4 and Table 5.5 demonstrate that by the combination of different web hole size and offset for each specimen a parametric study program was formed. For each loading condition a total of 150 specimens with offset web holes and 30 specimens having web holes located underneath bearing plate were modelled and analyzed in respective parametric study. As a result of parametric study, it is shown that web crippling strength reduction of rectangular hollow section having offset web hole is primarily affected by the diameter ratio (a/h) and offset distance ratio (x/h). For web holes located just

under the load bearing plate, reduction in strength is influenced only by ratio of web hole diameter to the flat depth of the web (a/h).

The effect of a/h for the specimen ITF-177.8 x 127 x 2.94 and ETF-177.8 x 127 x 2.94 is shown in Figure 5.5, Figure 5.6. It is found that like experimental testing results by increasing size of web hole in the form of increasing a/h value R value decreases. It shows a positive correlation between diameter of web holes and web crippling strength decrement. It is found that for specimen having offset web holes, for ITF loading conditions gap between different graphs are significantly higher as compared to ETF loading. It shows that for ITF loading reduction rate is more as compared to ETF loading, because of presence of web holes. It is associated with the reason that in case of ETF loading load is already acting at the edge of specimen and primary cause of failure is application of load at the end of specimen with little contribution towards failure from offset web holes. In case of ITF loading load acts at the mid length of specimen, and offset web holes contribute more towards web crippling failure. So, the reduction trend because of offset web holes is more in case of ITF loading than ETF loading. For web holes located centered under the bearing plate, the reduction rate for ETF loading is higher in comparison to ITF loading. It is due to the weakening of web at the end of section underneath the load because of web holes. In ETF loading end of the web gets weakened more as compared to that of ITF loading. So, ETF reduction is more in for the web holes located centered under the load bearing plate as compared to ITF loading.

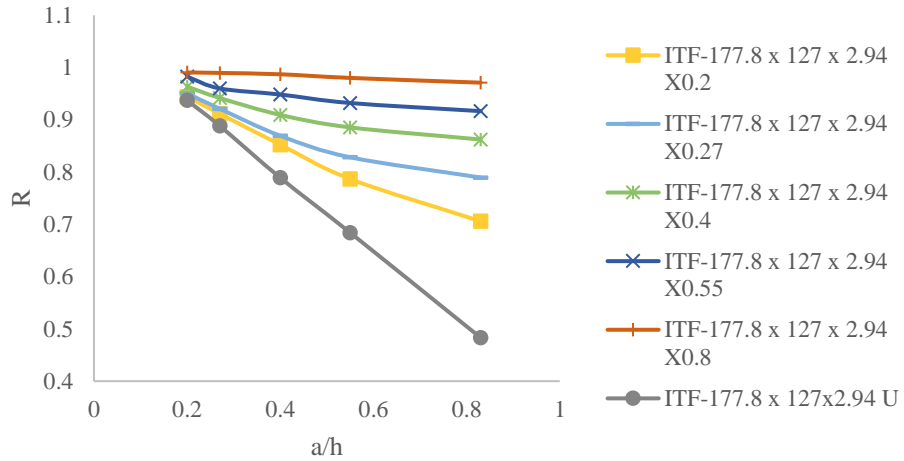


Figure 5.5: Strength reduction variation with size of web hole for ITF loading

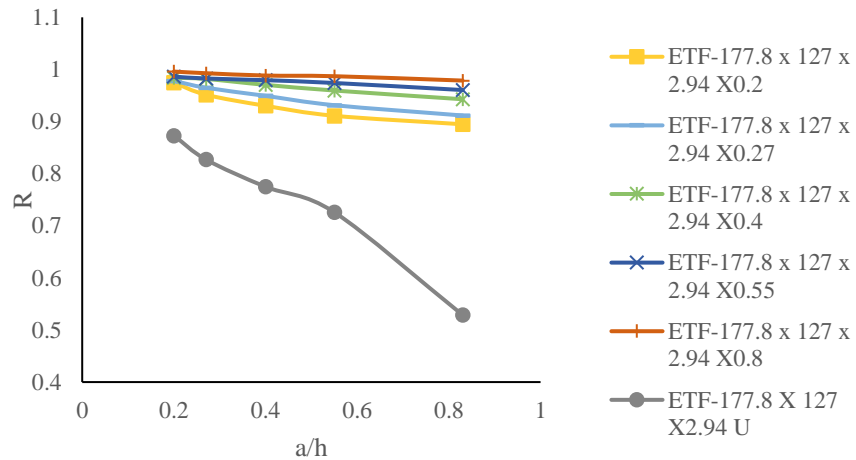


Figure 5.6 Strength reduction variation with size of web hole for ETF loading

Figure 5.7 and Figure 5.8 show the impact of offset distance ratio (x/h) on decrement of web crippling strength. The graphs between x/h vs R show that by increasing x/h values graphs move upward. It indicates that like experimental specimen as offset distance increases reduction in web crippling strength decreases. A negative correlation is observed between offset distance of web holes and web crippling strength decrement. It is

indicated that as web holes move away from loading bearing plate reduction in strength decreases. It indicates that web holes closer to the load, reduction trend in web crippling strength is significantly higher. For different specimen with web holes located at x/h value of 0.8, web crippling points for both the loading condition converges and come closer to R value of 1. It means that further the web holes from load, lesser susceptibility to web crippling because of web holes.

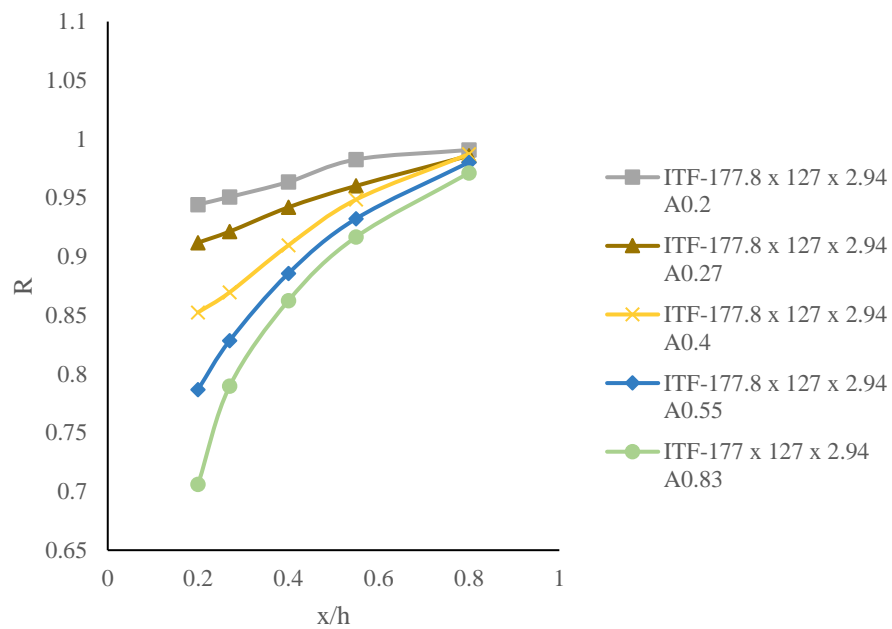


Figure 5.7: Strength reduction variation with position of web hole for ITF loading

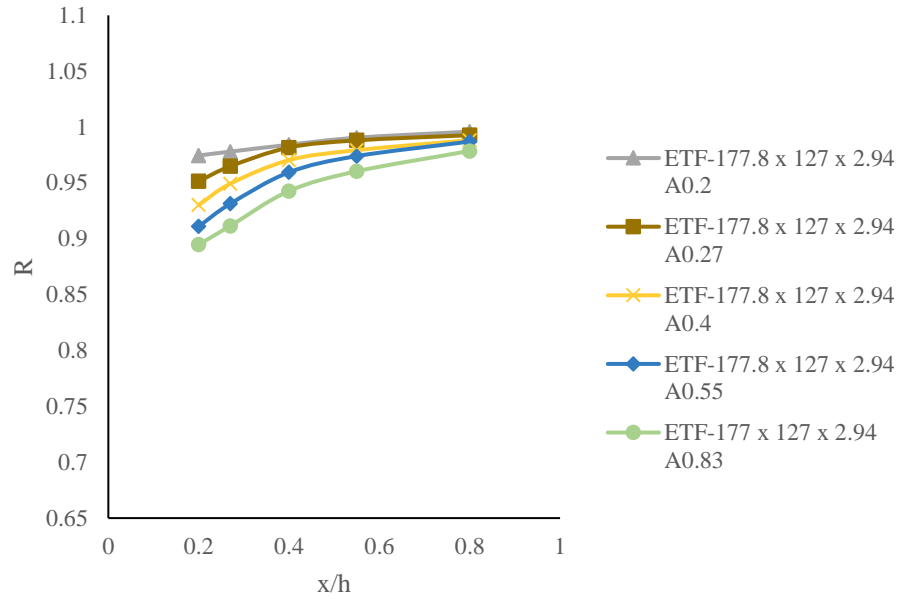


Figure 5.8: Variation of strength reduction with position of web hole for ETF loading

5.4 Web crippling strengths comparison with existing design rules

There are currently no codified guidelines to calculate the web crippling capacity of rectangular hollow sections with web holes in steel structure design standards. The web crippling strength design rules for the RHS without considering web holes are specified in AISC360 [11], AISI S100-16 [10], EC3 [33] and AS4100 [19]. These provisions are detailed in section 2.1 of the thesis.

Table 5.6: Comparisons between test and FE results of specimens without web holes with codified strengths subjected to ITF loading

Specimen	Dimensional ratios				$P_{\text{exp or FEA}}$	Comparison			
	h/t	N/t	r_{ext}/t	r_i/t		P/P _{AI}	P/P	P/P _E	P/P _A
						SC 360	AISI	C3	S 4100
ITF-101.6 x 76.2 x 4.25 WH	21.32	14.94	1.29	1.29	309.45	0.78	1.31	1.23	0.88
ITF-127 x 101.6 x 4.42 WH	26.70	14.37	1.02	1.02	335.48	0.90	1.30	1.23	0.83

ITF-127 x 101.6 x 11.81 WH	9.99	5.38	1.27	0.38	1485.9	0.56	0.75	0.71	1.12
ITF-177.8 x 127 x 2.94 WH	58.44	21.60	2.72	1.02	171.60	1.25	1.52	1.57	0.71
ITF-177.8 x 127 x 8.86 WH	19.39	7.17	0.56	0.34	1040.8	0.84	0.94	0.90	0.95
ITF-254 x 127 x 4.42 WH	55.43	20.36	1.81	1.02	273.70	0.89	1.06	1.10	0.58
ITF-254 x 127 x 7.39 WH	33.15	12.18	0.61	0.61	935.52	1.09	1.25	1.23	0.81
				P_m		0.90	1.16	1.14	0.84
				V_P		0.25	0.22	0.24	0.20
				β		1.37	2.13	1.95	1.37

Table 5.7: Comparisons between test and FE results of specimens without web holes with codified strengths subjected to ETF loading

Specimen	Dimensional ratios				$P_{\text{exp or FEA}}$	Comparison			
	h/t	N/t	r_{ext}/t	r_i/t		P/P_{AIS}	P/P_{AIS}	P/P_{EC}	P/P_{AS}
						C 360	I	3	4100
ETF-101.6 x 76.2 x 4.25 WH	21.32	14.94	1.29	1.29	199.37	0.88	2.57	2.60	0.79
ETF-127 x 101.6 x 4.42 WH	26.70	14.37	1.02	1.02	253.52	1.21	2.99	2.98	0.66
ETF-127 x 101.6 x 11.81 WH	9.99	5.38	1.27	0.38	966.39	0.65	1.45	1.51	1.08
ETF-177.8 x 127 x 2.94 WH	58.44	21.60	2.72	1.02	91.62	1.25	2.39	2.49	0.62
ETF-177.8 x 127 x 8.86 WH	19.39	7.17	0.56	0.34	683.98	1.02	1.81	1.90	0.89
ETF-254 x 127 x 4.42 WH	55.43	20.36	1.81	1.02	233.38	1.41	2.70	2.81	0.85
ETF-254 x 127 x 7.39 WH	33.15	12.18	0.61	0.61	589.18	1.27	2.37	2.42	0.66
				P_m		1.10	2.32	2.39	0.79
				V_P		0.24	0.23	0.22	0.21
				β		1.86	3.91	4.09	1.20

In Table 5.6 and Table 5.7 the web crippling strength of the sections without considering web holes is compared to the design strengths for ITF and ETF loading

conditions. For ITF and ETF specimens, the mean (P_m) ratios of $P/P_{AISC360}$ were 0.90 and 1.09 with the corresponding coefficient of variations (V_P) of 0.246 and 0.241, as well as reliability indices (β) of 1.36 and 1.85 respectively. This comparison shows that AISC360 provision about web crippling strength is a bit unconservative for ITF loading and in case of ETF loading it provides safe values of web crippling strength. But in case of stockier webs ($h/t = 9.99$ in this study) it provides very unconservative results for both loading conditions.

Considering AISI S100-16 [10] provisions, the mean ratios of P/P_{AISI} were 1.16 and 2.32, respective COVs were 0.223 and 0.227 along with that reliability indices were 2.12 and 3.91 respectively for ITF and ETF loadings. North American specifications provide safe and reliable results for both ITF and ETF loading conditions. But ETF provisions give greater conservatism. Like AISC360 [11] it also provides unconservative results for less slender webs in case of ITF loading condition.

For EC3 [33], the mean ratios P/P_{EC3} were 1.13 and 2.38, respective COVs were 0.241 and 0.215, and reliability indices were 1.94 and 4.09 for ITF and ETF loadings respectively. It indicates that EC3 provisions about web crippling strength of rectangular hollow section are safe and conservative, but in this case too, ETF provisions have higher conservatism. Like the former two provisions, AISC360 and AISI S100-16, EC3 also provides unconservative web crippling strength value for webs having low slenderness value for ITF loading.

For ITF and ETF specimens, in case of AS4100 [34] the mean ratios of P/P_{AS4100} were 0.84 and 0.79 with the respective COVs of 0.204 and 0.206, and reliability indices of 1.36 and 1.20 respectively. The AS4100 design provisions about web crippling capacity of RHS were quite unsafe and non-conservative for both loading conditions. It may be because of the reason that AS4100 provisions are very sensitive to the values of external radius (r_{ext}) of the section.

5.5 Proposed strength reduction factor

By the comparison of the web crippling strength of the specimens with the web crippling strength of specimens without web holes, it is discovered that diameter ratio (a/h) and offset distance ratio (x/h) are the basic parameters affecting the web strength of a specific rectangular hollow section with web holes. The only factor influencing the web crippling strength for specimen with a web hole directly under the load-bearing plate is a/h . Regression analyses are therefore carried out using the experimental data as well as the numerical outcomes of parametric research. For offset web holes multivariate linear regression analyses were conducted by considering a/h and x/h as independent variables, while reduction factor is considered as dependent variable. For web holes located centered under the load bearing plate, bivariate linear regression analyses are conducted, by taking a/h as independent variable while reduction factor as dependent variable. Based on these linear regression analyses, two reduction factors for each type of loading condition are proposed, R_P and R_{PU} . To obtain the web crippling strength of rectangular hollow section considering web holes, these reduction factors are to be multiplied with the strength of

section without consideration of web holes. In case of ITF loading condition reduction factor for

Offset web holes is

$$R_p = 0.90 - 0.11 \frac{a}{h} + 0.14 \frac{x}{h} \leq 1 \quad (5.1)$$

Web holes located just underneath load bearing plate is

$$R_{pU} = 1.05 - 0.65 \frac{a}{h} \leq 1 \quad (5.2)$$

For ETF loading condition reduction factor for

Offset web holes is

$$R_p = 0.91 - 0.075 \frac{a}{h} + 0.065 \frac{x}{h} \leq 1 \quad (5.3)$$

Web holes located just underneath load bearing plate is

$$R_{pU} = 0.96 - 0.61 \frac{a}{h} \leq 1 \quad (5.4)$$

5.6 Comparison of obtained reduction factor with proposed reduction factor

5.6.1 Graphical depiction of comparison

The comparison between the strength reduction value (R) obtained from experimental and numerical data and the proposed strength reduction factors (R_p and R_{pU}) allows for the evaluation of the accuracy of the suggested reduction factors. This assessment is conducted by calculating the ratio of R to R_p or R to R_{pU} . These ratios are plotted against the ratios of a/h as illustrated in Figure 5.9, Figure 5.10, Figure 5.11, Figure 5.12.

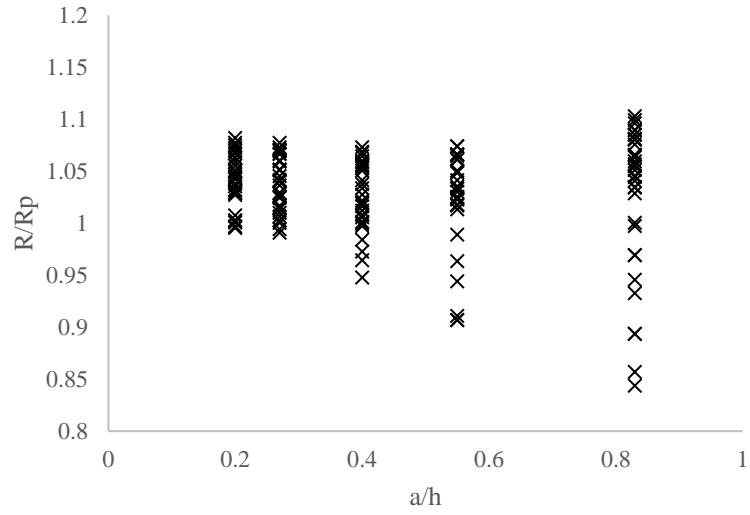


Figure 5.9: Comparison of strength reduction factors of specimens having offset web holes for ITF loading

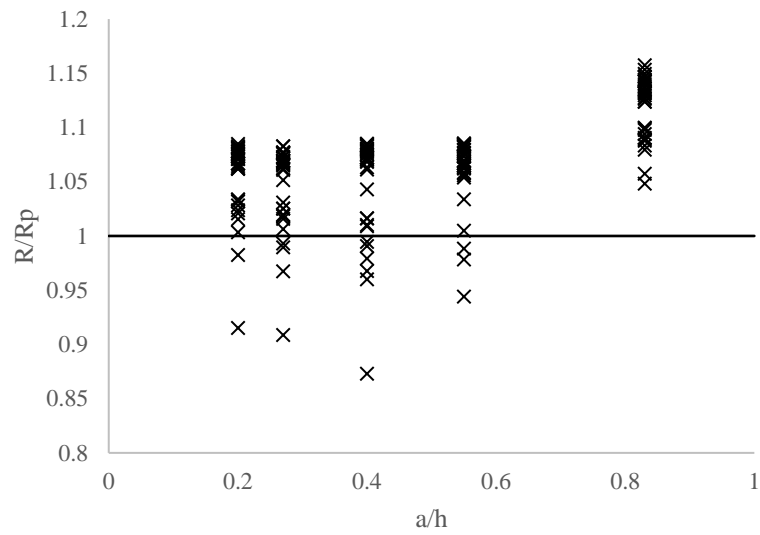


Figure 5.10: Comparison of strength reduction factors of specimens having offset web holes for ETF loading

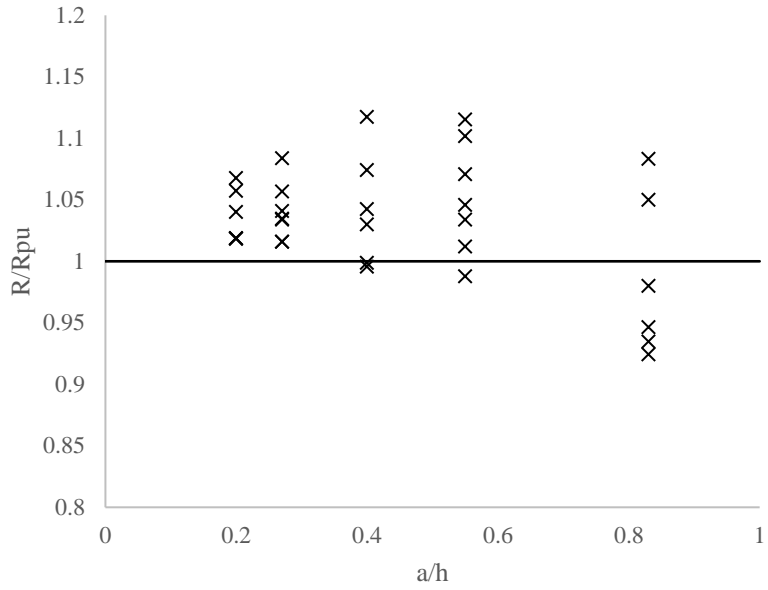


Figure 5.11: Comparison of strength reduction factors of specimen having web holes located underneath the load bearing plate for ITF loading

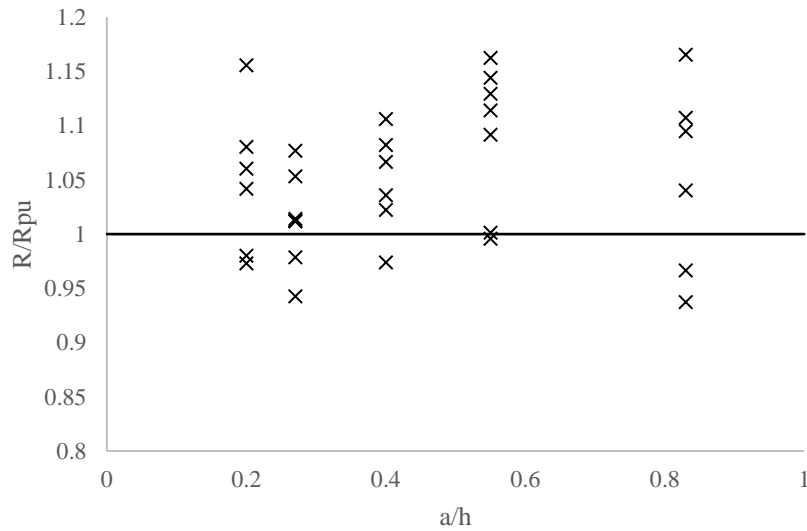


Figure 5.12: Comparison of strength reduction factors of specimen having web holes located underneath the load bearing plate for ETF loading

Graphical representation of R/R_P vs a/h and R/R_{PU} vs a/h shows that for all the four proposed reduction factors are mostly above the R/R_P and R/R_{PU} value of 1. These values

are above 1 but circulate in the near values of 1. These values indicate that proposed reduction factors are closely predicting the web crippling reduction because of size and offset distance of web holes.

To check the accuracy of proposed reduction factors for each specimen are plotted between h/t and R/R_p as shown in Figure 5.13 and Figure 5.14. In this graph h/t value is a representative value of each specimen. From the above charts of h/t vs R/R_p , it is shown that for ITF loading almost for every specimen, most of the R/R_p values are above 1. Each value lies in the near radius of 1 value of R/R_p , indicating the accuracy of proposed reduction factor for each specimen. For ETF loading, for most of the specimens R/R_p values are above one but for the specimen having h/t value of 26.70 some of the values are below one, but all the values are much closer to one. So, considering the accuracy, safety and conservatism of proposed design factors, these reduction factors are opted to encounter the reduction in web crippling strength because of size and offset distance of web holes.

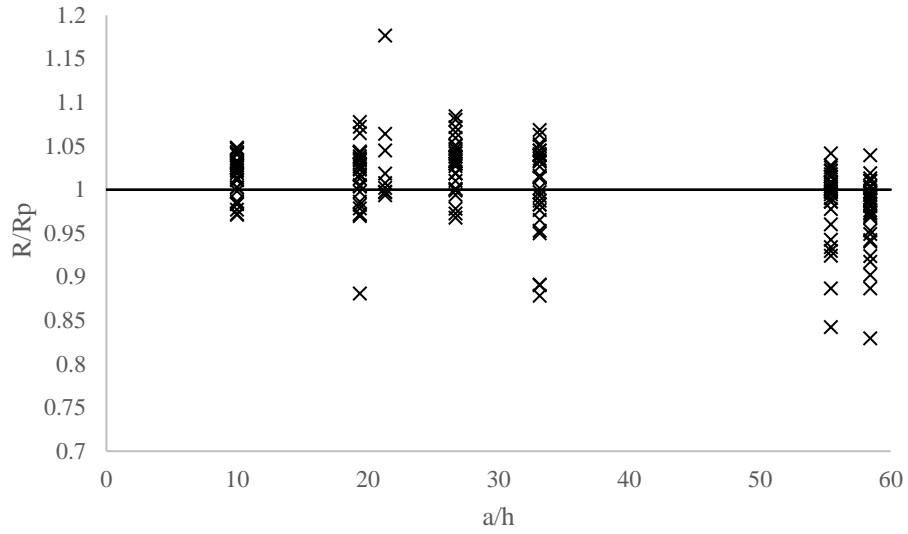


Figure 5.13 Reduction factor comparisons vs slenderness ratio for ITF loading

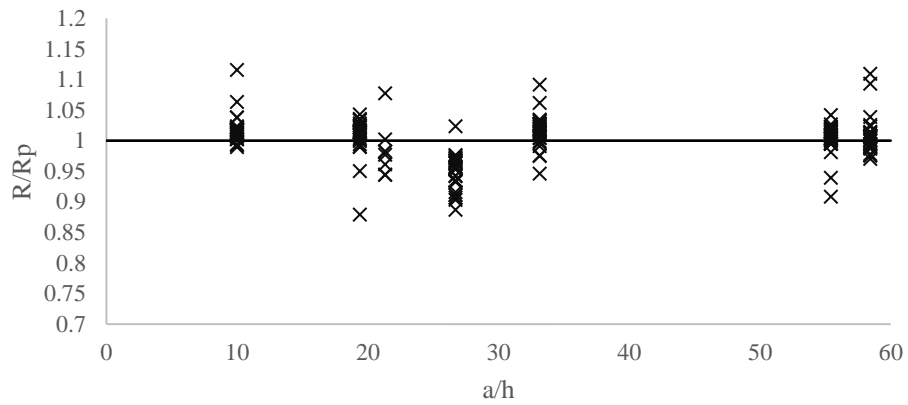


Figure 5.14 Reduction factor comparisons vs slenderness ratio for ETF loading

5.6.2 Comparison using statistical analyses

After confirming the accuracy of proposed reduction factors using graphical representation, statistical analyses are conducted too, to check the accuracy of proposed reduction factors. During statistical analysis mean values of R/R_p and coefficient of

variation are calculated. Table 5.8 shows the value of parameters involved in statistical analysis. These parameters are mean values of ratio (P_m), coefficient of variation (V_P), reliability index (β) and resistance factor (ϕ). It is found that all the mean values of R/R_P are very close to 1 and coefficient of variation ranges between 0.044 to 0.072. Hence these results of statistical analyses indicate that these reduction factors equations (R_P and R_{PU}) predict the reduced web crippling strength well for both types of loadings. These reduction factors are providing accurate measurements of reduction of strength by incorporating web hole size and offset distance in both cases, for offset web holes and web holes centered underneath the load bearing plate.

Table 5.8: Statistical analyses of compared actual strength reduction factor with proposed strength reduction factor for (a) offset web holes (b) web holes positioned underneath load bearing plate

(a)			(b)		
Statistical parameters	R/R _P		Statistical parameters	R/R _{PU}	
	ITF	ETF		ITF	ETF
P_m	1.03	1.06	P_m	1.03	1.05
V_P	0.044	0.045	V_P	0.055	0.072
β	2.68	2.79	β	2.68	2.70
ϕ	0.90	0.90	ϕ	0.90	0.90

5.7 Reliability analysis

Accuracy of proposed reduction factor is determined by graphical and statistical analysis. To evaluate the reliability level proposed reduction factors of rectangular hollow steel sections considering size and position of web holes, reliability analyses are performed. The reliability analyses provide reliability checks and assurance that extent of reliability of proposed equations of reduction factors. Reliability index (β) provides the representative

value to classify the reliability criteria of proposed design equations. The safety of design is quantified by its relative measure. AISC-360 [11] recommends the 2.6 as the lower bound value for the intended reliability index of steel structural members. If the reliability index value is above 2.6, the recommended design provision is deemed dependable and reliable. AISI S100-16 [10] provides additional insight on reliability analysis. In the reliability analysis, as defined by the ASCE standard the load combination of 1.2DL + 1.6LL was considered. Where DL is dead load and LL is the live load. The reliability index is calculated as

$$\beta = \frac{\ln\left(\frac{C_\phi M_m F_m P_m}{\Phi_c}\right)}{\sqrt{V_M^2 + V_F^2 + C_P V_P^2 + V_Q^2}}$$

The parameters involved in reliability analyses are taken from of the AISI S100-16 [10] for compression members. The values of different factors and coefficients used are

- Coefficient of calibration, $C_\phi = 1.52$,
- Material factor's mean Value, $M_m = 1.10$,
- Fabrication factor's mean value, $F_m = 1.00$,
- Material factor's coefficient of variation, $V_M = 0.1$,
- Fabrication factor's coefficient of variation, $V_F = 0.05$,
- Load effect's coefficient of variation $V_Q = 0.21$,
- P_m is the mean value for a particular set of data,
- V_P is the coefficient of variation of results,
- C_P is the correction factor and is determined by a formula as given.

$$C_P = \frac{\left(1 + \frac{1}{n}\right)^m}{m-2} \quad (5.5)$$

n = total number of considered tests and

m = degrees of freedom = n-1

- ϕ is the resistance factor and taken as 0.90 for hot-rolled steel sections web crippling failure as per AISC-360 [11].

The value of reliability indices for each detail is given in Table 5.6, Table 5.7 and Table 5.8. Reliability indices values for all proposed reduction factors are well above the target value of 2.6, which indicates that design provisions presented as reduction factors are reliable.

CHAPTER 6: CONCLUSIONS AND FUTURE RECOMMENDATIONS

6.1 Conclusions

Experimental and numerical investigations have been carried out to examine the web crippling strength of rectangular hollow steel sections by considering web holes. A set of 20 experiments were conducted under ITF and ETF loading conditions. To assess the impact of diameter and offset distance of web hole on the web crippling capacity of the rectangular hollow section, specimens were prepared with varying diameters (a) and offset distances (x) of the web holes. On the basis of the the findings of this study, subsequent conclusions are drawn.

1. FEM results were compared against experimental results. The mean ratios of experimental web crippling strengths to the finite element web crippling strength were 0.98 and 1.03 for ITF and ETF loadings respectively. It shows that finite element models agree well with experimental findings.
2. After the verification of numerical strengths and failure modes with experimental strengths and failure modes, a comprehensive parametric study was conducted on six different cross sections of rectangular hollow steel sections. In this parametric study, parameters considered were diameter ratio (a/h) and offset distance ratio (x/h) for offset web holes. For web holes located centered underneath the load bearing plate only diameter ratio is considered.

3. From the findings of experimental and parametric study, it is observed that a positive correlation exists between a/h and web crippling strength reduction. It indicates that by increasing size of web hole reduction in web crippling strength will be more. Also there exists a negative correlation exists between x/h and strength reduction. It shows that by moving web hole away from load, decrement in web crippling strength gets reduced.
4. For offset web holes, reduction trend in web crippling strength for ITF loading is more as compared to ETF loading. A maximum of 6.2% more reduction is observed for ITF loading.
5. While considering web holes located centered under the bearing plate, reduction trend in web crippling strength obtained under ETF load case is significantly higher as compared to ITF loading. In ETF loading, up to 9.95 % more reduction is observed as compared to ITF loading.
6. For both types of loadings, design recommendations in the form of strength reduction factor were made.
7. The accuracy and conservatism of proposed reduction factors is evaluated using graphical and statistical analyses. As a result of these analyses, the values obtained from these reduction factors are found to be accurate and conservative.
8. Reliability levels of these design recommendations were assessed using reliability analyses. It is shown that these recommendations are safe and reliable.

6.2 Future Research Recommendations

For the similar future researches, it is recommended that

1. Web crippling capacity of rectangular hollow steel sections by considering web holes under one flange loadings (IOF and EOF) should be investigated.
2. The impact of circular web openings on web crippling of RHS with flanges of the section fastened to bearing plates can also be determined.
3. The effect of non-circular web openings like rectangular, filleted corner rectangular or any geometrically practical shape openings, on web crippling capacity of RHS can be evaluated.

REFERENCES

- [1] P. McEntee, “Steel Moment Frames – History and Evolution ,” Feb. 2009.
- [2] Steel LLC., “A Brief History of Steel Construction”, June 2018
- [3] Z. A. Siddiqui, “*Steel Structures*”, 4th ed. Help Civil Engineering Publisher, 2017.
- [4] J. C. McCormac and S. F. Csernak, “*STRUCTURAL STEEL DESIGN*”, 5th ed. Pearson Higher Education, 2012.
- [5] Y. Chen, X. Chen, and C. Wang, “Tests and behavior of hot-rolled channel steel sections subjected to web crippling,” *J Constr Steel Res*, vol. 117, pp. 101–114, 2016, doi: 10.1016/j.jcsr.2015.10.008.
- [6] J. Lu, H. Liu, Z. Chen, and X. Liao, “Experimental investigation into the post-fire mechanical properties of hot-rolled and cold-formed steels,” *J Constr Steel Res*, vol. 121, pp. 291–310, Jun. 2016, doi: 10.1016/j.jcsr.2016.03.005.
- [7] D. T. Phan *et al.*, “Design optimization of cold-formed steel portal frames taking into account the effect of building topology,” *Engineering Optimization*, vol. 45, no. 4, pp. 415–433, Apr. 2013, doi: 10.1080/0305215X.2012.678493.
- [8] American Institute of Steel Construction, *Steel Construction Manual*, 14th ed. 2011.
- [9] X. Yun and L. Gardner, “Numerical modelling and design of hot-rolled and cold-formed steel continuous beams with tubular cross-sections,” *Thin-Walled Structures*, vol. 132, pp. 574–584, Nov. 2018, doi: 10.1016/j.tws.2018.08.012.
- [10] American Iron and Steel Institute (AISI), “*North American Specification for the Design of Cold-Formed Steel Structural Members*”, 16th ed. 2016.
- [11] American Institute of Steel Construction (AISC), “*Specification for Structural Steel Buildings*”, AISC 360-16. 2016.
- [12] R. M. Lawson and S. J. Hicks, “Design of Composite Beams with Large web openings,” 2011.
- [13] P. D. McKenna and R. M. Lawson, “*Design of Steel Framed Building for Services Integration*”. Steel Construction Institute, Silwood Park, Ascot.
- [14] “Service integration,” *SteelConstruction.info*. s

- [15] K. F. Chung, T. C. H. Liu, and A. C. H. Ko, "Investigation on Vierendeel mechanism in steel beams with circular web openings," *J Constr Steel Res*, vol. 57, no. 5, pp. 467–490, May 2001, doi: 10.1016/S0143-974X(00)00035-3.
- [16] I. Fareed, W. Somadasa, K. Poologanathan, S. Gunalan, V. Beatini, and S. Sivabalan, "Web Crippling Behaviour of Cold-formed Stainless Steel Beams with Non-Circular Web Opening," *ce/papers*, vol. 3, no. 3–4, pp. 937–942, Sep. 2019, doi: 10.1002/cepa.1170.
- [17] M. Elgaaly and R. K. Salker, "Web crippling under local compressive edge loading," in *4th National Steel Construction Conference, Washington, USA: AISC.*,
- [18] J. He and B. Young, "Web crippling design of cold-formed steel built-up I-sections," *Eng Struct*, vol. 252, p. 113731, Feb. 2022, doi: 10.1016/j.engstruct.2021.113731.
- [19] E. Kanthasamy *et al.*, "Web Crippling Behaviour of Cold-Formed High Strength Steel Unlipped Channel Beams," *Buildings*, vol. 12, no. 3, p. 291, Mar. 2022, doi: 10.3390/buildings12030291.
- [20] L. Sundararajah, M. Mahendran, and P. Keerthan, "Web crippling experiments of high strength lipped channel beams under one-flange loading," *J Constr Steel Res*, vol. 138, pp. 851–866, Nov. 2017, doi: 10.1016/j.jcsr.2017.06.011.
- [21] M. Macdonald, M. A. Heiyantuduwa Don, M. Kotełko, and J. Rhodes, "Web crippling behaviour of thin-walled lipped channel beams," *Thin-Walled Structures*, vol. 49, no. 5, pp. 682–690, May 2011, doi: 10.1016/j.tws.2010.09.010.
- [22] G. Davies and J. A. Packer, "Analysis of web crippling in a rectangular hollow section," 1987.
- [23] F. Zhou and B. Young, "Design and tests of cold-formed high strength stainless steel tubular sections subjected to web crippling," *Welding in the World*, vol. 50, no. SPEC. ISS., pp. 258–264, 2006.
- [24] K. J. Zhan, H. T. Li, Z. H. Fan, and B. Young, "Web crippling tests of cold-formed stainless steel tubular sections at elevated temperatures," *Eng Struct*, vol. 304, Apr. 2024, doi: 10.1016/j.engstruct.2024.117452.
- [25] J. He and B. Young, "Behaviour of cold-formed steel built-up I-sections with perforated web under localized forces," *J Constr Steel Res*, vol. 190, 2022, doi: 10.1016/j.jcsr.2022.107129.
- [26] A. M. Yousefi, B. Samali, I. Hajirasouliha, Y. Yu, and G. C. Clifton, "Unified design equations for web crippling failure of cold-formed ferritic stainless steel unlipped channel-sections with web holes," *Journal of Building Engineering*, vol. 45, p. 103685, Jan. 2022, doi: 10.1016/j.job.2021.103685.

- [27] R. A. LaBoube, W. W. Yu, S. U. Deshmukh, and C. A. Uphoff, “Crippling capacity of web elements with openings,” *Journal of Structural Engineering*, vol. 125, no. 2, pp. 137–141, 1999, doi: 10.1061/(ASCE)0733-9445(1999)125:2(137).
- [28] J. E. Langan, R. A. LaBoube, and Yu. W. W., “Structural Behavior of Perforated Web Elements of Cold-Formed Steel Flexural Members Subjected to Web Crippling and a Combination of Web Crippling and Bending,” Rolla, 1994.
- [29] A. Uzzaman, J. B. P. Lim, D. Nash, J. Rhodes, and B. Young, “Web crippling behaviour of cold-formed steel channel sections with offset web holes subjected to interior-two-flange loading,” *Thin-Walled Structures*, vol. 50, no. 1, pp. 76–86, 2012, doi: 10.1016/j.tws.2011.09.009.
- [30] A. Uzzaman, J. B. P. Lim, D. Nash, J. Rhodes, and B. Young, “Effect of offset web holes on web crippling strength of cold-formed steel channel sections under end-two-flange loading condition,” *Thin-Walled Structures*, vol. 65, pp. 34–48, Apr. 2013, doi: 10.1016/j.tws.2012.12.003.
- [31] F. Zhou and B. Young, “Web crippling of aluminium tubes with perforated webs,” *Eng Struct*, vol. 32, no. 5, pp. 1397–1410, 2010, doi: 10.1016/j.engstruct.2010.01.018.
- [32] H.-T. Li and B. Young, “Tests of cold-formed high strength steel tubular sections undergoing web crippling,” *Eng Struct*, vol. 141, pp. 571–583, Jun. 2017, doi: 10.1016/j.engstruct.2017.03.051.
- [33] European Committee for Standardization, “*Eurocode 3 - Design of steel structures - Part 1-3: General rules - Supplementary rules for cold-formed members and sheeting*”, vol. Part 1-3. 2006.
- [34] Council of Standards Australia, “*AS 4100:2020 Steel structures*”, AS 4100:2020. 2020.
- [35] T. M. Roberts, “Slender Plate Girders Subjected to Edge Loading,” *Proceedings of the Institution of Civil Engineers*, vol. Part 2, Sep. 1981.
- [36] M. Elgaaly and R. Salker, “Web Crippling Under Edge Loading,” in *Proceedings, National Steel Construction Conference*, Washington, DC : AISC, 1991.
- [37] M. R. Kaczinski, C. R. Schneider, R. J. Dexter, and L.-W. Lu, “Local Web Crippling of Unstiffened Multi-Cell Box Sections,” in *Proceedings of the ASCE Structures Congress '94 Atlanta*, New York: ASCE, 1994, pp. 343–348.
- [38] G. Winter and R. H. J. Pian, “Crushing Strength of Thin Steel Webs,” *Cornell Bulletin* 35, vol. Part 1, Apr. 1946.
- [39] L. Zetlin, “Elastic Instability of Flat Plates Subjected to Partial Edge Loads,” *Journal of the Structural Division*, vol. 81, Sep. 1955.

- [40] N. Hetrakul and Yu. W. W, "Structural Behavior of Beam Webs Subjected to Web Crippling and a Combination of Web Crippling and Bending," Rolla, Jun. 1978.
- [41] Yu. W. W, "Web Crippling and Combined Web Crippling and Bending of Steel Decks," Rolla, Apr. 1981.
- [42] C. Santaputra, M. B. Parks, and W. W. Yu, "Web Crippling of High Strength Cold-Formed Steel Beams," *Journal of Structural Engineering*, vol. 115, no. 10, Oct. 1989.
- [43] B. H. Bhakta, R. A. LaBoube, and W. W. Yu, "The Effect of Flange Restraint on Web Crippling Strength," Rolla, Mar. 1992.
- [44] D. E. Cain, LaBoube R.A., and Yu. W. W, "The Effect of Flange Restraint on Web Crippling Strength of Cold-Formed Steel Z- and I-Sections," Rolla, May 1995.
- [45] S. Wu, Yu. W. W, and LaBoube R. A., "Strength of Flexural Members Using Structural Grade 80 of A653 Steel (Web Crippling Tests)," 1997.
- [46] B. A. Wing and Schuster R.M., "Web Crippling of Decks Subjected to Two-Flange Loading," in *Proceedings of the Sixth International Specialty Conference on Cold-Formed Steel Structures*, Rolla: University of Missouri-Rolla, Nov. 1982.
- [47] K. Prabakaran, "Web Crippling of Cold-Formed Steel Sections," University of Waterloo, Waterloo, Canada, 1993.
- [48] R. R. Gerges, "Web Crippling of Single Web Cold-Formed Steel Members Subjected to End One-Flange Loading," University of Waterloo, Waterloo, Canada, 1997.
- [49] R. R. Gerges and R.M. Schuster, "Web Crippling of Members Using High- Strength Steels," in *Proceedings of the Fourteenth International Specialty Conference on Cold-Formed Steel Structures*, Rolla: University of Missouri-Rolla, 1998.
- [50] K. Prabakaran and Schuster R.M., "Web Crippling of Cold-Formed Steel Members," in *Proceedings of the Fourteenth International Specialty Conference on Cold-Formed Steel Structures*, Rolla: University of Missouri-Rolla, Oct. 1998.
- [51] B. Beshara, "Web Crippling of Cold-Formed Steel Members," University of Waterloo, Waterloo, Canada, 1999.
- [52] B. Beshara and R. M. Schuster, "Web Crippling of Cold-Formed C- and Z-Sections," in *Proceedings of the Fifteenth International Specialty Conference on Cold-Formed Steel Structures*, Rolla: University of Missouri-Rolla, Oct. 2000.
- [53] B. Young and G. J. Hancock, "Web Crippling Behaviour of Cold-Formed Unlipped Channels," in *Proceedings of the Fourteenth International Specialty Conference on Cold-Formed Steel Structures*, Rolla: University of Missouri-Rolla, Oct. 1998.

- [54] C. A. Uphoff, “Structural Behavior of Circular Holes in Web Elements of Cold-Formed Steel Flexural Members Subjected to Web Crippling for End-One-Flange Loading,” University of Missouri-Rolla, Rolla, 1996.
- [55] S. U. Deshmukh, “Behavior of Cold-Formed Steel Web Elements With Web Openings Subjected to Web Crippling and a Combination of Bending and Web Crippling for Interior-One-Flange Loading,” University of Missouri-Rolla , Rolla, 1996.
- [56] American Institute of Steel Construction, *STEEL CONSTRUCTION MANUAL*, 14th ed. 2015.
- [57] ASTM International, “ASTM E8, Standard Test Methods for Tension Testing of Metallic Materials,” in *ASTM Standards*, 2016.
- [58] Dassault Systèmes Simulia Corp., “ABAQUS/Standard User’s Manual.” 2017.
- [59] A. M. Howatson, P. G. Lund, and J. D. Todd, *Engineering Tables and Data*. Springer Science & Business Media, 2012.
- [60] H. Qiu and T. Inoue, “Evolution of Poisson’s Ratio in the Tension Process of Low-Carbon Hot-Rolled Steel with Discontinuous Yielding,” *Metals (Basel)*, vol. 13, no. 3, Mar. 2023, doi: 10.3390/met13030562.
- [61] X. Yun and L. Gardner, “Numerical modelling and design of hot-rolled and cold-formed steel continuous beams with tubular cross-sections,” *Thin-Walled Structures*, vol. 132, pp. 574–584, Nov. 2018, doi: 10.1016/j.tws.2018.08.012.
- [62] X. Yun, L. Gardner, and N. Boissonnade, “The continuous strength method for the design of hot-rolled steel cross-sections,” *Eng Struct*, vol. 157, pp. 179–191, Feb. 2018, doi: 10.1016/j.engstruct.2017.12.009.
- [63] P. Natário, N. Silvestre, and D. Camotim, “Web crippling failure using quasi-static FE models,” *Thin-Walled Structures*, vol. 84, pp. 34–49, Nov. 2014, doi: 10.1016/j.tws.2014.05.003.
- [64] M. Bock and E. Real, “Strength curves for web crippling design of cold-formed stainless steel hat sections,” *Thin-Walled Structures*, vol. 85, pp. 93–105, Dec. 2014, doi: 10.1016/j.tws.2014.07.021.
- [65] H.-T. Li and B. Young, “Web crippling of cold-formed ferritic stainless steel square and rectangular hollow sections,” *Eng Struct*, vol. 176, pp. 968–980, Dec. 2018, doi: 10.1016/j.engstruct.2018.08.076.
- [66] R. J. M. Pijpers and H. M. Slot, “Friction coefficients for steel to steel contact surfaces in air and seawater,” *J Phys Conf Ser*, vol. 1669, no. 1, p. 012002, Oct. 2020, doi: 10.1088/1742-6596/1669/1/012002.

[67] P. Natário, N. Silvestre, and D. Camotim, “Web crippling failure using quasi-static FE models,” *Thin-Walled Structures*, vol. 84, pp. 34–49, Nov. 2014, doi: 10.1016/j.tws.2014.05.003.

[68] B. Janarthanan, M. Mahendran, and S. Gunalan, “Numerical modelling of web crippling failures in cold-formed steel unlipped channel sections,” *J Constr Steel Res*, vol. 158, pp. 486–501, Jul. 2019, doi: 10.1016/j.jcsr.2019.04.007.